

Online Appendix:

“Income Growth and the Distributional Effects of Urban Spatial Sorting”

Appendix A U-Shaped Sorting Pattern

In this section, we detail the construction of the U-Shape pattern in sorting documented in Figure 1 in the main text. We also highlight the robustness of the U-Shape pattern within detailed demographic groups.

Appendix A.1 Main U-Shape Figure

Figure 1 of the main text summarizes the Engel curve for residing downtown. It shows the relative propensity of families to reside downtown by income, and its evolution over time. The stylized facts in this figure are based on data from the 1970, 1990, and 2000 U.S. Censuses, as well as from the 2012-2016 American Community Surveys (ACS). We refer to the 2012-2016 pooled ACS data as the 2014 ACS. We use census tract level data published by the National Historical Geographic Information System (NHGIS). All data are interpolated to constant 2010-boundary tracts and 2014-boundary CBSAs using the Longitudinal Tract Data Base (LTBD). We complement Census tables with microdata from the Integrated Public Use Micro-data Series (Ruggles et al., 2018), adjusted for top-coding using the generalized Pareto method. We use the 1% IPUMS sample in 1970, and the 5% IPUMS samples in 1990, 2000, and 2012-2016. In what follows, all income measures are CPI-adjusted to 1999 dollars. We provide a detailed discussion of this data (including our top-coding procedure) below in Appendix C.

With this data, we measure the location choice of households with differing levels of income. Central to our analysis is the notion of the dense urban center of a CBSA, which we refer to as the “downtown,” “urban areas,” or “urban center” interchangeably throughout the paper. Our baseline definition of an urban center is as follows. In each CBSA, we focus on the CBSA’s main city, and within this main city on its city center. We define the city center of each CBSA using the locations provided by Holian and Kahn (2012), who use the coordinates returned by Google Earth for a search of each CBSA’s principal city. We then classify as downtown the set of tracts closest to the city center that accounted for 10 percent of the CBSA’s population in 2000. This defines a spatial boundary of downtown, which we keep constant across all years. Each point represents the share of families, in a given Census income bracket, who reside downtown in a given year – normalized by the share of all families who reside downtown that year. This normalization allows for the abstraction of the suburbanization of the population as a whole over this period due to general population growth. The share of families at all income levels that live downtown was 0.1 in 2000 (by construction) but was 0.17 in 1970 and 0.08 in 2014. The x-axis features the median family income for that bracket in the same year, in 1999 dollars, computed using IPUMS micro

data. The number of points on the graph is limited by the number of income brackets reported by the Census for tract-level information.

Appendix A.2 U-Shape with Demographic Controls

We note that these facts are robust to the definition of an urban area, CBSA sub-samples, the choice of price deflator, and the use of household income rather than family income. One may think that these U-shape patterns reflect demographic characteristics that are correlated with income, and/or that the changes in the U-shape pattern over time simply reflect demographic shifts that are correlated with income and that took place between 1990 and 2014. In this section, we replicate Figure 1 showing normalized urban shares by income bracket, but controlling for demographic characteristics.

Unlike Figure 1 that uses Census tables from the 100 largest CBSAs, here we use our 27 CBSAs with constant urban geography, which allows us to control for demographic characteristics of households. We create demographic control dummies for race, age, family type, and nationality of birth.³⁷ For age, we construct 5-year age buckets. For family type, we define four categories: Unmarried - No Children, Married - No Children, Youngest Child < 5, and Youngest Child > 5. For race, we use the IPUMS definitions.³⁸ For nationality of birth, we define two categories: native born and foreign born.

To compute urban shares within each income bracket without demographic controls, we estimate the following equation, separately in 1990 and in 2014:

$$\text{UrbanWeight}_i = c + \sum_{k \in K} \beta_k \text{IncomeDummy}_{ki}, \quad (\text{A.1})$$

where UrbanWeight_i is the urban weight of household i , which equals 1 if the household is assigned entirely to the urban area of its CBSA.³⁹ IncomeDummy_{ki} is a dummy equal to 1 if household i is in income bracket k .⁴⁰ The fitted values from this regression are urban shares within each income bracket. To normalize these shares relative to the average household, we divide the fitted value for each income bracket, $\hat{c} + \hat{\beta}_k$, by a weighted average of all fitted values, where each fitted value is weighted by the total number of households in that income bracket. Plotting these normalized fitted values against median income within each income bracket replicates Figure 1 in the paper,

³⁷The age, race, and nationality at birth are that of the head of household. The youngest age for a head of household with nonzero income is 15.

³⁸We have to merge three categories in 2014 so the definitions are consistent across both periods. These three categories are ‘Other race’ ‘Two major races’ and ‘Three or more major races’. We correspond all of these to the 1990 definition ‘Other race’. Hispanic is a separate variable in IPUMS. For this analysis, we do not distinguish whether a person is hispanic or not.

³⁹We use a weight instead of a 0/1 dummy because we only know household location at the PUMA level, and some PUMAs span both the urban and suburban areas.

⁴⁰We assign each household into 100 evenly log-spaced household income brackets. We adopt this methodology so brackets are directly comparable between 1990 and 2014, and to ensure large enough population counts in higher income brackets. We merge the bottom 61 brackets with income below \$10,000, and then we drop all income between \$200,000 and \$400,000 that is heavily impacted by topcoding in IPUMS. See Appendix C for further discussion. Our results are robust to different methods of adjusting for topcodes.

but using IPUMS data for our 27 constant geography CBSAs instead of Census tables.

To compute urban shares that control for demographic characteristics, first denote each group of controls (age, household type, race, birth status) by g , and each category within a group by d (e.g., 30-34 year olds). The estimating equation becomes:

$$\text{UrbanWeight}_i = c + \sum_{k \in K} \beta_k \text{IncomeDummy}_{ki} + \sum_{g \in G} \sum_{d \in D} \gamma_{gd} \text{DemoDummy}_{igd}, \quad (\text{A.2})$$

where DemoDummy_{igd} is equal to 1 if household i is in category d within group of controls g . To obtain urban shares within each income bracket k that control for demographic characteristics, we compute fitted values of equation A.2 under the assumption that demographic shares within each income brackets are exactly representative of the demographic shares within the total population. Under this assumption, fitted urban shares are equal to:

$$c + \widehat{\beta}_k + \sum_{g \in G} \sum_{d \in D} \text{SharePop}_{gd} \times \widehat{\gamma}_{gd},$$

where SharePop_{gd} is the share of total population in each category d (e.g., share of 30-34 year olds).

Figure A.1 shows normalized urban shares for each income bracket in 1990 and 2014. The left-hand plots shows estimates from equation (A.1) (without demographic controls) and the right-hand plot shows estimates from equation (A.2) (with demographic controls.)

Our key finding is that controlling for demographics makes the U-shape even more pronounced at the top of the income distribution, in both 1990 and 2014. The regression results from equation A.2 show what drives this finding. In Table A.1, column 1 and 2 show the coefficient on each demographic group dummy in 1990 and 2014, column 3 and 4 show the correlation of each demographic group dummy with household income in 1990 and 2014, and column 5 and 6 show the share of the population within each demographic group. The table shows that there is almost an exact correspondence between the demographic groups that are most suburbanized, wealthiest, and largest. This explains why the urban share of high income households is larger once we control for demographics; high income households would be even more urbanized if they weren't also white, middle-aged, and with older children, all of which are suburbanized demographic categories. These first order correlations hold in both 1990 and 2014, so the uptick in the U-shape from 1990 to 2014 largely persists after adding demographic controls.

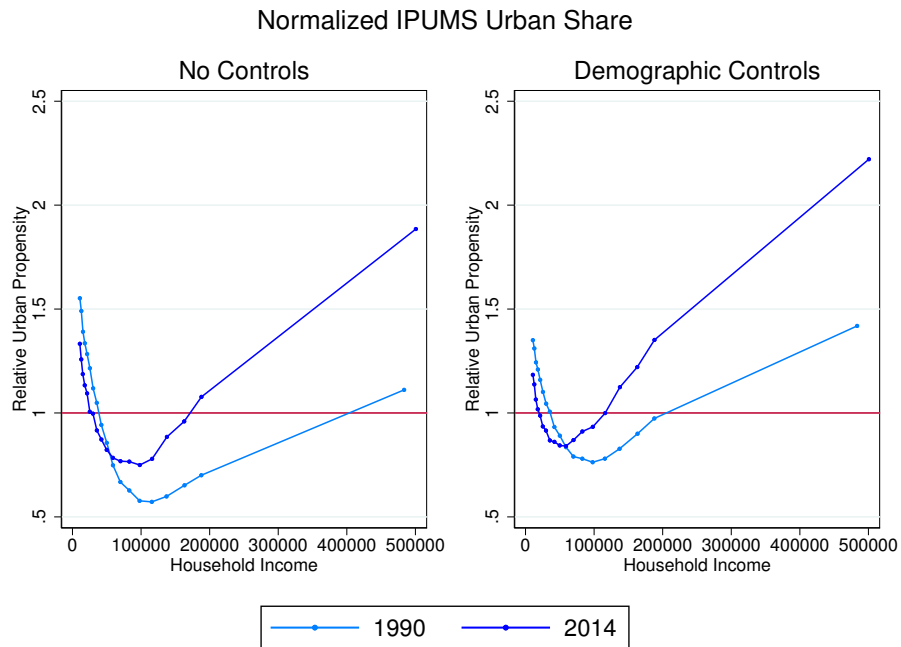
To further assess whether the U-shape patterns that we document are specific to certain demographic categories, in Figure A.2 we plot normalized urban shares separately by demographic category within each group. To get large enough samples, we further aggregate age (25-34, 35-44, 45-64, 65+), and race (we keep "white" and "black". The "other" category is comprised mostly of Asian, Indigeneous, or multiethnic households.) Remarkably, we find a U-shape pattern, and an urbanization of the richest households from 1990 to 2014 in each category within each group of demographic characteristics.

Table A.1: Coefficients on Demographic Control Dummies in 1990 and 2014

Variable	Coefficient		Correlation with HH Income		Share of Pop Within Group	
	1990	2014	1990	2014	1990	2014
Age < 24 (omitted)	.	.	-0.114	-0.091	0.047	0.032
Age 25-29	-0.001	0.021	-0.051	-0.051	0.101	0.071
Age 30-34	-0.008	0.004	0.006	-0.005	0.123	0.091
Age 35-39	-0.011	-0.026	0.049	0.030	0.118	0.092
Age 40-44	-0.019	-0.046	0.098	0.051	0.109	0.098
Age 45-49	-0.020	-0.059	0.118	0.063	0.088	0.102
Age 50-54	-0.021	-0.069	0.099	0.062	0.071	0.106
Age 55-59	-0.019	-0.072	0.067	0.049	0.066	0.100
Age 60-64	-0.018	-0.071	0.010	0.014	0.068	0.087
Age 65-69	-0.024	-0.076	-0.063	-0.014	0.067	0.072
Age 70-74	-0.029	-0.078	-0.096	-0.044	0.055	0.052
Age 75-99	-0.032	-0.083	-0.109	-0.061	0.044	0.038
Age 80-84	-0.037	-0.087	-0.098	-0.066	0.027	0.029
Age 85+	-0.034	-0.094	-0.087	-0.081	0.017	0.030
Native Born (omitted)	.	.	0.041	0.048	0.847	0.752
Foreign Born	0.038	0.027	-0.041	-0.048	0.149	0.248
Unmarried-No children (omitted)	.	.	-0.288	-0.244	0.343	0.380
Married-No children	-0.056	-0.058	0.111	0.128	0.209	0.200
Youngest Child ≤ 5	-0.073	-0.104	0.012	0.031	0.138	0.105
Youngest Child > 5	-0.062	-0.076	0.189	0.125	0.310	0.315
White (omitted)	.	.	0.150	0.113	0.780	0.690
Black	0.147	0.058	-0.148	-0.132	0.141	0.158
Native American	0.048	0.037	-0.014	-0.017	0.004	0.004
Chinese	0.089	0.042	0.011	0.023	0.010	0.021
Japanese	0.034	0.034	0.016	0.010	0.004	0.003
Other Asian	0.014	-0.001	0.019	0.053	0.020	0.049
Other Race (including mixed raced)	0.121	0.038	-0.073	-0.070	0.041	0.074

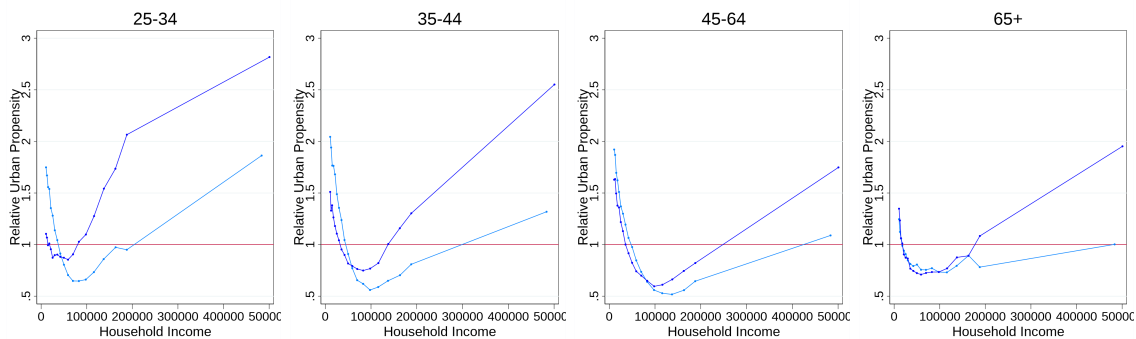
Note: Columns 1 and 2 report the coefficients from equation (A.2) for years 1990 and 2014 with all demographic controls included. The standard errors are very small and not shown. Columns 3 and 4 show the pairwise correlation of each demographic control dummy and household income. Columns 5 and 6 report the total share of population falling into each demographic category.

Figure A.1: Impact of Demographic Controls on Relative Urbanization by Income

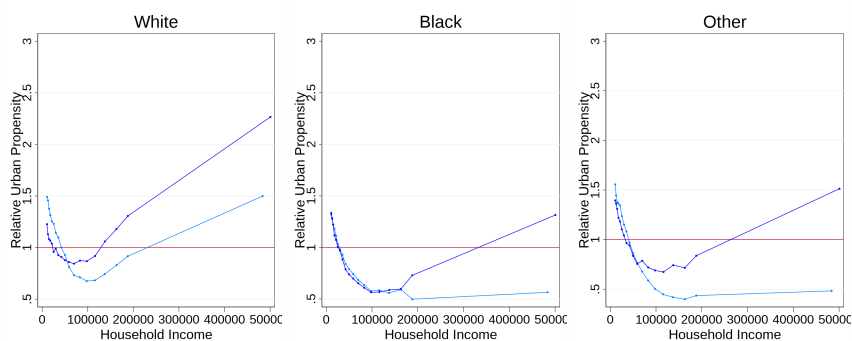


Note: This figure shows urban shares normalized by the aggregate urban share in each year with and without demographic controls. The left plot shows the coefficients from equation (A.1). The right plot shows the coefficients from equation (A.2). We drop household with income below \$10,000 and between \$200,000 and \$400,000. IPUMS data from 1990 and 2014 in 27 CBSAs with constant urban areas.

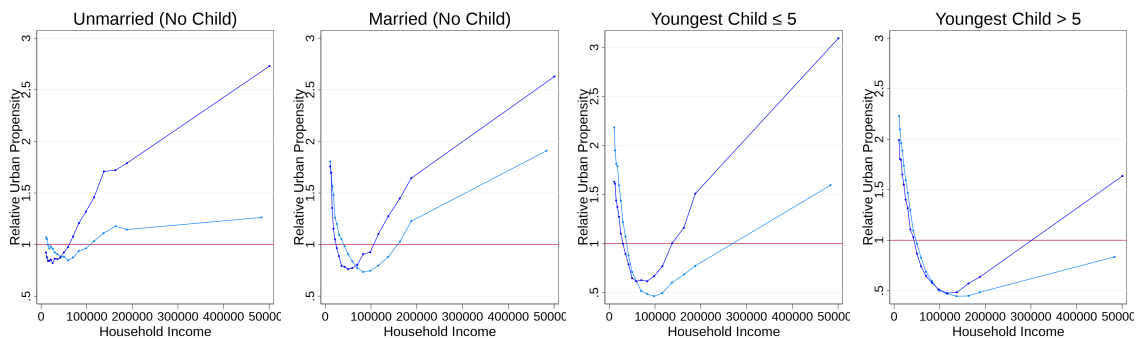
Figure A.2: Normalized Urban Shares by Demographic Categories in 1990 and 2014
 Panel A: Age



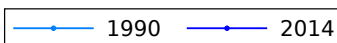
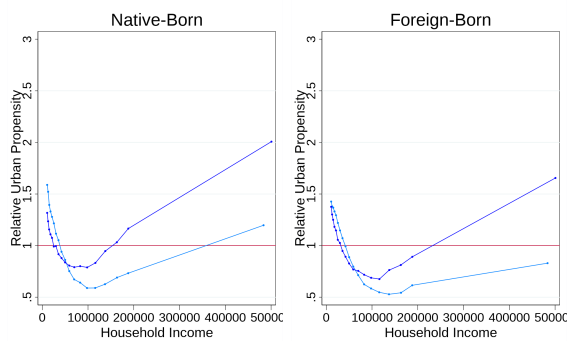
Panel B: Race



Panel C: Family Type



Panel D: Foreign Status



Note: This figure shows normalized urban shares from equation (A.1), plotted separately for each demographic category. The right plot shows the coefficients from equation (A.2). We drop household with income below \$10,000 and between \$200,000 and \$400,000. IPUMS data from 1990 and 2014 in 27 CBSAs with constant urban areas.

Appendix B Model Appendix

Appendix B.1 Income Elasticity of Housing consumption

Neighborhoods differ in the size and quality of their housing units, driven by the quality shifter k_{nj} that in turn impacts housing prices p_{nj} (see equation (14)), but housing is homogeneous within a neighborhood. Therefore, in the model, variation in housing spending patterns across income groups arises solely from variation in the fraction of households who choose neighborhoods of various types. Despite this simple setup, we show now that the model is able to capture salient features of housing consumption in the data, even with only two quality levels like in our empirical application. Denoting with $\bar{p}(w) \equiv \sum_{n,j} \lambda_{nj}(w) p_{nj}$ the average expenditure on housing for households of income w , the income elasticity of housing consumption in the model is:

$$\frac{\partial \log \bar{p}(w)}{\partial \log w} = \rho \frac{w}{\bar{p}(w)} \sum_{nj} \left(p_{nj}^h - \bar{p}(w) \right) \lambda_{nj}(w) \nu_{nj}(w), \quad (\text{B.3})$$

where $\nu_{nj}(w) = (w - p_{nj})^{-1}$. This income elasticity $\frac{\partial \log \bar{p}(w)}{\partial \log w}$ is strictly positive as soon as the city has more than one type of neighborhoods to choose from (and would be trivially 0 otherwise).

Proof. If there is only one type of neighborhood, one can factorize $\nu(w)$ and get that:

$$\frac{\partial \log \bar{p}(w)}{\partial \log w} = \rho \nu(w) \frac{w}{\bar{p}(w)} \sum_{nj} \left(p_{nj}^h - \bar{p}(w) \right) \lambda_{nj}(w) = 0,$$

by definition of \bar{p} . If there are several types of neighborhoods, note that $\nu_{nj}(w)$ increases with p_{nj} . Therefore, $\text{cov} \left(p_{nj}^h \lambda_{nj}(w) - \bar{p}(w) \lambda_{nj}(w), \nu_{nj}(w) \right) > 0$ for any w . The result follows. \square

Finally, the housing expenditure share $\frac{\bar{p}(w)}{w}$ decreases with income, as in the data. We show in Figure 6 that our quantified model captures the empirical fact that, within cities, the expenditure share on housing decreases, as a function of income.

Appendix B.2 Closing the Model: Neighborhood Development

A developer of neighborhood r of type nj faces total operating cost $\int_w \lambda_r(w) k_{n,j} R_n dL(w)$ to serve its demand, for revenues $\int_w \lambda_r(w) p_{n,j} dL(w)$, so that its operating profits are:

$$\pi_r = \left[\int_w \lambda_r(w) dL(w) \right] (p_r - k_{n,j} R_n) \quad (\text{B.4})$$

Among households with income w , the share who locates in a particular neighborhood r of type (n, j) is $\lambda_r(w) = \lambda_{nj}(w) \lambda_{r|nj}(w)$, where the notation $\lambda_{r|nj}$ indicates the share of workers who choose neighborhood r conditional on choosing a neighborhood of quality j in location n . Given

the structure of the idiosyncratic preference shocks, the conditional probability of choosing r among other (n, j) choices is:⁴¹

$$\lambda_{r|nj}(w) = \frac{V_r(w)^\gamma}{\sum_{r' \in \mathcal{R}(nj)} V_{r'}(w)^\gamma} = \frac{V_r(w)^\gamma}{V_{nj}(w)^\gamma}, \quad (\text{B.5})$$

where $V_{nj}(w)$ is defined in (4) and $V_r(w)$ is the inclusive value of neighborhood r :

$$V_r(w) = ((1 - \tau_{n(r)})w - p_r)B_{nj(r)}. \quad (\text{B.6})$$

The probability $\lambda_{nj}(w)$ that the neighborhood chosen is of type (n, j) is given by (3). Plugging in the expression for λ_r as a function of price and taking the developer's first order condition for profit maximization leads to the following pricing formula:

$$p_r = \frac{\gamma}{\gamma + 1} k_{nj} R_n + \frac{1}{\gamma + 1} \mathcal{W}_{nj}(p_r), \quad (\text{B.7})$$

where $\mathcal{W}_{nj}(p) = \frac{\int_w (1 - \tau_n)((1 - \tau_n)w - p)^{-1} \delta_{nj}(w) w dL(w)}{\int_w ((1 - \tau_n)w - p)^{-1} \delta_{nj}(w) dL(w)}$ with $\delta_{nj}(w) = 1\{(1 - \tau_n)w - p > 0\}$.

By symmetry, all neighborhoods of type (n, j) have the same price in equilibrium, which we denote as p_{nj} , given in (14). Finally, under free entry, the number of developers entering location n at quality j becomes:

$$N_{nj} = \frac{1}{f_{nj}} \left[\int_w \lambda_{nj}(w) (p_{nj} - k_{nj} R_n) dL(w) \right]. \quad (\text{B.8})$$

Appendix B.3 Model Extensions

Demand for Neighborhoods We detail here the model equations in the full model that accounts for the additional building blocks of section 2.3. The net income of household w in neighborhood r located in location n is:

$$m_n(w) = (1 - \tau_n)w + \chi(w) - T_n(w), \quad (\text{B.9})$$

Given the utility function in (15) and the provision of public amenities in (19), the indirect utility of a household ω who locates in neighborhood r of type n, j is:

$$\max_r (m_n(w^\omega) - p_r^h) (P_{nj}^a)^{-\alpha} B_{nj}^o (G_n)^\Omega b_r^\omega$$

where p_r^h is housing price in r and P_{nj}^a is the price index for consumption of amenities for someone

⁴¹In equilibrium, all neighborhoods are symmetric within type, so that $\lambda_{r|nj}(w) = \frac{1}{N_{nj}}$.

living in a neighborhood of type nj ,

$$P_{nj}^a = \left(\sum_{n',j'} N_{n'j'} \beta_{jj'} \left(d_{nn'}^\delta P_{n'j'}^a \right)^{1-\sigma} \right)^{\frac{1}{1-\sigma}}. \quad (\text{B.10})$$

The inclusive value of living in neighborhood r for a household with wage w is:

$$V_r(w) = (m_n(w) - p_r^h) (P_{nj}^a)^{-\alpha} B_{nj}^o (G_n)^\Omega \quad (\text{B.11})$$

Supply of Neighborhoods Given CES demand for amenities, developers price amenities at a constant markup over marginal costs, that is:

$$p_r^a = \frac{\sigma}{\sigma - 1} k_{n(r)j(r)}^a R_{n(r)}, \quad (\text{B.12})$$

so that in equilibrium, operational profits made on the amenities market by a developer of type (n, j) is:

$$\pi_{n,j}^a = \frac{\alpha}{\sigma} \int_w \frac{\lambda_{n,j}(w) (m_n(w) - p_{n,j}^h)}{N_{nj}} dL(w)$$

and the land used by amenities of type (n, j) , K_{nj}^a , is pinned down by:

$$R_n K_{nj}^a = \frac{\sigma - 1}{\sigma} \alpha^a \int_w \lambda_{n,j}(w) (m_n(w) - p_{n,j}^h) dL(w). \quad (\text{B.13})$$

Similarly, land used by housing in neighborhoods of type nj is pinned down by:

$$R_n K_{nj}^h = \int_w \lambda_{n,j}(w) k_{n,j}^h R_n dL(w). \quad (\text{B.14})$$

The land market clearing condition is therefore:

$$K_n^0 (R_n)^{\epsilon_n} = \sum_j (K_{nj}^h + K_{nj}^a). \quad (\text{B.15})$$

As in the baseline model, the price of housing (now with a superscript h , p_r^h) is pinned down by profit maximization of developers on the housing market given demand. Under free entry, the number of developers entering location n at quality j becomes:

$$N_{nj} = \frac{1}{f_{nj}} \left[\int_w \lambda_{n,j}(w) \left(p_{nj}^h - k_{n,j}^h R_n + \frac{\alpha}{\sigma} (m_n(w) - p_{nj}^h) \right) dL(w) \right]. \quad (\text{B.16})$$

Appendix B.4 Computing Counterfactuals

We describe here how to compute a counterfactual equilibrium for a different income distribution $L'(w)$, conditional on (i) an initial calibration corresponding to the income distribution $L(w)$, and

(ii) on the model elasticities $\{\rho, \gamma, \epsilon_n, \sigma, \alpha, \tau_n\}$. The information necessary to perform this step are the calibrated values at the initial equilibrium for $\{\lambda_{n,j}(w), p_{n,j}^h, S_{n,j}^{mk}\}$, where $L_{n,j}$ is the total population living in neighborhoods of type $\{n, j\}$ in the initial equilibrium, i.e.:

$$L_{n,j} = \int L(w) \lambda_{n,j}(w) dw,$$

and where $S_{n,j}^{mk}$ is the share of amenity expenditures of households living in a neighborhood of type nj spent on amenities consumed in a neighborhood (m, k) . These shares are taken from the smartphone data.

We write a counterfactual equilibrium in changes relative to the initial equilibrium, denoting by $\hat{x} = \frac{x'}{x}$ the relative change of the variable x between the two equilibria. The counterfactual equilibrium is the solution to the following set of equations for $\{(p_{n,j}^h)'\}$, $\lambda'_{n,j}(w)$, $L'_{n,j}$ –or, equivalently, their “hat” values.

First, given (B.15), changes in housing costs are given by:

$$\hat{R}_n = \left(\sum_j s_{n,j}^h \hat{R}_n \hat{L}_{n,j} + s_{n,j}^a \hat{R}_n \hat{K}_{n,j}^a \right)^{\frac{1}{1+\epsilon_n}}, \quad (\text{B.17})$$

where we have used the notation $s_{n,j}^i$ to denote the shares of land used by usage $i \in \{h, a\}$ and quality j within location n in the initial equilibrium, that is:

$$s_{n,j}^i = \frac{R_n K_{n,j}^i}{\sum_{j',i'} R_n K_{n,j'}^{i'}},$$

which we compute from the calibrated values of $R_n K_{n,j}^a$ using equation B.13, as well as the calibrated values of $R_n K_{n,j}^k$ using equation B.14.⁴² Note that $\hat{L}_{n,j} = \frac{\int \lambda'_{n,j}(w) dL'(w)}{\int \lambda_{n,j}(w) dL(w)}$ while $\hat{R}_n \hat{K}_{n,j}^a = \frac{\int \lambda'_{n,j}(w) (w - (p_{n,j}^h)') dL'(w)}{\int \lambda_{n,j}(w) (w - p_{n,j}^h) dL(w)}$, where $\lambda'_{n,j}(w)$ is unknown and a solution of the system of equations described here, while the counterfactual distribution of income $L'(w)$ is taken as given.

Second, the housing prices in the new equilibrium are defined by⁴³:

$$\left(p_{n,j}^h \right)' = \frac{\gamma}{\gamma + 1} k_{n,j}^h R_n \hat{R}_n + \frac{1}{\gamma + 1} \mathcal{W}'_{n,j} \left((p_{n,j}^h)' \right), \quad (\text{B.18})$$

where the function $\mathcal{W}'_{n,j}(p)$ is defined by:

$$\mathcal{W}'_{n,j}(p) = \frac{\int_w \Lambda'_{n,j}(p, w) [(1 - \tau_n)w + \chi(w)'] L'(w) dw}{\int_w \Lambda'_{n,j}(p, w) L'(w) dw}, \quad (\text{B.19})$$

⁴²We have $\sum_{i,j} s_{n,j}^i = 1$ for $n = D$ or S and $\sum_{m,k} S_{n,j}^{mk} = 1$, for $n = D, S$ and $j = H, L$.

⁴³Note that $k_{n,j}^h R_n$ is known in the initial equilibrium using equation B.7 and the known variables $p_{n,j}^h, \lambda_{n,j,r}(w), L(w)$

with $\Lambda'_{n,j}(p, w) = \frac{\lambda'_{n,j,r}(w)}{[(1-\tau_n)w + \chi(w) - p]}$. Note here that τ_n and $\chi(w)$ are assumed constant between the two equilibria.

Third, the change in overall neighborhood attractiveness $\tilde{B}_{n,j}$ is driven in particular by changes in number of neighborhoods of different types $\hat{N}_{n,j}$ and the change in density \hat{K}_n . Starting from the definition of \tilde{B}_n , simple algebraic manipulations lead to:

$$\hat{B}_{n,j} = \hat{N}_{n,j}^{\frac{1}{\gamma}} \left(\hat{P}_{n,j}^a \right)^{-\alpha} \hat{G}_n^\Omega \quad (\text{B.20})$$

In this expression, the change in the number of neighborhoods is given by:

$$\hat{N}_{n,j} = s_{n,j}^{\pi,h} \hat{L}_{n,j} \frac{\left(p_{n,j}^h \right)' - k_{n,j}^h R'_n}{p_{n,j}^h - k_{n,j}^h R_n} + \left(1 - s_{n,j}^{\pi,h} \right) \frac{X'_{n,j} - \left(p_{n,j}^h \right)' L'_{n,j}}{X_{n,j} - p_{n,j}^h L_{n,j}},$$

where we define $X_{n,j}$ to be total income in n, j :

$$X_{n,j} = \int_w \lambda_{n,j}(w) w dL(w),$$

and we have defined the initial shares in profits made on the housing (vs amenities) market:

$$s_{n,j}^{\pi,h} = \frac{\left(p_{n,j}^h - k_{n,j}^h R_n \right) L_{n,j}}{\left(p_{n,j}^h - k_{n,j}^h R_n \right) L_{n,j} + \frac{\alpha}{\sigma} \left(X_{n,j} - p_{n,j}^h L_{n,j} \right)}.$$

Furthermore, given Equation B.10, the change in the price index for amenities in a neighborhood of type n, j is:

$$\left(\hat{P}_{n,j}^a \right)^{1-\sigma} = \sum_{j'n'} S_{n,j}^{n'j'} \hat{N}_{n'j'} \hat{d}_{nn'}^{-\delta} \left(\hat{R}_{n'} \right)^{1-\sigma},$$

where $S_{n,j}^{m,k}$ is the calibrated share of expenditure on amenities spent on neighborhood of type m, k for households living in neighborhood of type n, j , as defined in 18.

To solve for $\hat{d}_{nn'}$, we make use of the simple geometric assumption that representative distance $d_{nn'}$ changes like the square root of the corresponding land area K_n .

Third, change in tax levied is:

$$\hat{G}_n = \frac{\int L'(w) \left(\sum_j \lambda'_{n,j}(w) \right) T'_n(w) dw}{\int L(w) \left(\sum_j \lambda_{n,j}(w) \right) T_n(w) dw}.$$

where $T'_n(w)$ is the tax scheme in the counterfactual equilibrium, possibly different (exogeneously so) from the one in the reference equilibrium.

Finally, the counterfactual location choice of workers can be simply expressed as a function of initial location choices $\lambda_{n,j}$, changes in neighborhood quality and prices defined above, and changes

in income, which we take as an exogenous input to the counterfactual. Specifically, changes in location choices are given by:

$$\widehat{\lambda}_{n,j}(w) = \frac{\widehat{B}_{n,j}^\rho [w(1 - \tau_n) + \chi'(w) - p'_r]^\rho}{\widehat{V}^\rho(w) [w(1 - \tau_n) + \chi'(w) - p_r]^\rho}, \quad (\text{B.21})$$

In parallel, we get the change in welfare given by:

$$\widehat{V}^\rho(w) = \sum_{n,j} \widehat{B}_{n,j}^\rho \frac{[(1 - \tau_n)w + \chi'(w) - p'_r]^\rho}{[(1 - \tau_n)w + \chi(w) - p_r]^\rho} \lambda_{n,j}(w), \quad (\text{B.22})$$

Values for $\{p'_{n,j}, \lambda'_{n,j}(w), L'_{n,j}, R'_{n,j}\}$ are the solutions of equations (B.17)-(B.21) that define a counterfactual equilibrium of the economy corresponding to an alternative distribution of income $L'(w)$ in the city.

Appendix B.5 Welfare

The model lends itself naturally to welfare analysis. Given the setup of the model, the representative welfare of households with wage w is given by:

$$V(w) = \left(\sum_{n',j'} V_{n',j'}^\rho(w) \right)^{1/\rho}. \quad (\text{B.23})$$

where V_{nj} is the inclusive value of all neighborhoods of type (n, j) , i.e.:

$$V_{nj}(w) = \left(\sum_{r' \in \mathcal{B}(nj)} V_{r'}(w)^\gamma \right)^{\frac{1}{\gamma}}, \quad (\text{B.24})$$

where V_r is the inclusive value of living in neighborhood r as given in B.11. In the full quantitative model, this is:

$$V_{nj}(w) = N_{nj}^{\frac{1}{\gamma}} V_r = B_{nj} N_{nj}^{\frac{1}{\gamma}} (P_{nj}^a)^{-\alpha} (m_n(w) - p_{nj}^h). \quad (\text{B.25})$$

Appendix C Data Appendix

In this appendix, we discuss our data sources, we provide additional detail on variable construction, and we illustrate the downtown areas of some CBSAs.

Appendix C.1 Data Sources and Sample Descriptions

This subsection details the data sources used in our various empirical analyses. We also discuss how we adjust our income data for topcoding in the IPUMS data.

Appendix C.1.1 Census Data and ACS Data

Census Tract Data For our work at the neighborhood level, we assemble a database of constant 2010 geography census tracts using the Longitudinal Tract Data Base (LTDB) and data from the National Historical Geographic Information System (NHGIS) for the 1970-2000 censuses and the 2012-2016 ACS. In each of the censuses from 1970 to 2000, some tracts are split or consolidated and their boundaries change to reflect population change over the last decade. The LTDB provides a crosswalk to transform a tract level variable from 1970 to 2000 censuses into 2010 tract geography. This reweighting relies on population and area data at the census block level, which is small enough to ensure a high degree of accuracy. We combine these reweighted data with the 2012-2016 ACS data, which already uses 2010 tract boundaries.

CBSA Definitions Core Based Statistical Areas (CBSAs) refer collectively to metropolitan and micropolitan statistical areas. CBSAs consist of a core area with substantial population, together with adjacent communities that have a high degree of economic and social integration with the core area. We assign 2010 census tracts to CBSAs based on 2014 CBSA definitions. Our model estimation sample consists of the 100 metropolitan area CBSAs with the largest population in 1990s.

IPUMS Data PUMA geography is also not constant from 1990 to 2014, so we use a crosswalk between PUMAs (Public-Use Microdata Areas) and CBSAs in each year to link each PUMA to a CBSA. To construct constant downtowns from PUMAs across years, we follow the methodology in (Couture and Handbury, 2017). We first intersect PUMA geographies in 1990 and 2014 with our constant downtown geography described in the main text, defined out of tracts closest to the city center accounting for 10 percent of a CBSA's population in 2000. PUMAs generally intersect with both the urban and suburban area of a CBSA, so we assign an urban weight to each PUMA equal to the percentage of that PUMA's population falling within the urban area (i.e., downtown) of that CBSA. We compute the urban and suburban population of each PUMA using the population of all census blocks whose centroid falls in a given area.

In most of the 100 CBSAs, PUMAs are too large to accurately represent downtowns. We therefore enforce an inclusion criteria where we only keep CBSAs for which 60% of the urban

population lives in PUMAs whose population is at least 60% urban. Under this restriction, we find a set of 27 CBSAs for which we can define urban areas in 1990 and 2014.

Topcoding in IPUMS Data IPUMS data is topcoded by income component. Household and family income reported in the IPUMS data is sum of total individual income for all members of the household or family. Total individual income is the sum of income components where each component has a unique topcode. Table C.2 shows each of the income components that contribute to total individual income and their respective topcodes for 1990 and 2014.

Table C.2: Topcoded Income Components Contributing to Total Individual Income

1990			2000+		
Variable	Description	Topcode (nominal)	Variable	Description	Topcode (nominal)
INCWAGE	Pre-tax wage and salary income	\$140,000	INCWAGE	Pre-tax wage and salary income	99.5th Percentile in State
INCBUS	Non-farm business and/or professional practice income	\$90,000	INCBUS00*	Business and farm income and/or professional practice income	99.5th Percentile in State
INCFARM	Farm	\$54,000	INCSS	Social security and disability	Not Topcoded
INCSS	Social security and disability	\$17,000	INCWELFR	Other government assistance	Not Topcoded
INCWELFR**	Other government assistance	10,000	INCSUPP	Supplementary Security Income	Not Topcoded
INCINVST	Rents, interests, dividends, etc.	\$40,000	INCINVST	Rents, interests, dividends, etc.	99.5th Percentile in State
INCRETIR	Retirement income other than social security	\$30,000	INCRETIR	Retirement income other than social security	99.5th Percentile in State
INCOTHER	Income not included above	\$20,000	INCOTHER	Income not included above	99.5th Percentile in State

* 1990 equivalent is INCBUS + INCFARM

** 2014 equivalent is INCWELFR + INCSUPP

In 1990, component topcodes are the same across all states. Table C.3 shows the percent of all units impacted by topcoding for each component for individuals, households, and families. For households and families, we conservatively assume that any household or family whose reported component level income is above the person-level topcode is subject to topcoding for that component. The last row of the table shows the percent of total aggregate income impacted where we apply the individual-level topcode for wages.

In the 2012-2016 ACS, component topcodes vary both across states and year. State-specific topcodes for wages range from \$105,000 to \$280,000 in 1999 dollars. Because of this high variance, we allow each state to retain a state-specific topcode: the minimum topcode in 1999 dollars across the 5 years of ACS. Table C.4 shows the percent of income impacted by topcodes for different components and units of observation. The last row of the table shows the percent of total aggregate income impacted where we apply the state specific individual-level topcode for wages.

Armour et al. (2016) apply a type I Pareto distribution to estimate the tail of topcoded income

Table C.3: Percent of Income Impacted by Topcoded Components in 1990

Variable	Person	Household	Family
incwage	0.60%	1.39%	1.66%
incbus	3.70%	4.25%	4.62%
incfarm	2.79%	3.28%	3.48%
incss	0.73%	3.67%	5.60%
incwelfr	3.18%	5.80%	6.83%
incinvest	2.11%	2.98%	3.18%
incretir	3.20%	4.15%	5.08%
incother	2.28%	2.51%	2.43%
TOTAL	0.62%	1.78%	2.28%

Note: This table shows the percent of income at or above the topcode value in 1990 among the set of observations where income is non-missing and greater than \$0.

Table C.4: Percent of Income Impacted by Topcoded Components in 2014

Variable	Person	Household	Family
incwage	1.2%	3.5%	4.5%
incbus	3.7%	4.4%	5.1%
incinvest	3.6%	4.6%	5.2%
incretir	3.5%	5.6%	7.2%
incother	3.4%	4.0%	4.0%
TOTAL	1.5%	4.1%	5.8%

Note: This table shows the percent of income at or above the topcode value in 2014 among the set of observations where income is non-missing and greater than \$0. The topcode value is set at the minimum topcode in each state across the five years of ACS (2012-2016).

in survey data. Equation C.26 shows their formula for estimating the pareto shape parameter α_{tsn} for time period t , state s , and area n .⁴⁴

$$\widehat{\alpha}_{tsn} = \frac{M_{tsn}}{T_{tsn} \ln(X_{Ts}) + \sum_{x_{m_{tsn}} \leq x_i < x_{T_{tsn}}} \ln(x_i) - (M_{tsn} + T_{tsn}) \ln(x_{m_{tsn}})} \quad (\text{C.26})$$

M_{tsn} is the number of households or families with earnings between the lower cutoff $x_{m_{tsn}}$ and the censoring point $x_{T_{tsn}}$. In 1990, we assign the censoring point as the topcode for a single-wage household adjusted to 1999 dollars (\$188,160). In 2014, for state s we choose censoring point as the topcode for a single-wage household for the year with the lowest topcode of the 5 years surveyed. T_{tsn} is the number of households with income at or above censoring point $x_{T_{tsn}}$. We choose the lower cutoff $x_{m_{tsn}}$ as the 95% income in state s for period t and area n . This is consistent with Armour et al. (2016).⁴⁵

Piketty et al. (2017) further improve upon the constant parameter estimate. Using individual tax data, they find that a single Pareto distribution cannot sufficiently explain the tail of an income distribution. In the U.S. context, the relationship between the Pareto parameter and income has become increasingly U-shaped over time. This would suggest that the simple Pareto as outlined in Armour et al. (2016) not only underestimates the fatness of the right tail of the income distributions but does so especially in 2014 relative to 1990. Piketty et al. (2017) develop a methodology to construct generalized Pareto curves that allow the pareto coefficient to vary with income. We use the R package *gpinter* that Piketty et al. (2017) developed to estimate the generalized Pareto curves for each state s , area n , and period t .^{46,47}

We combine the income distribution observed in the IPUMS data below the topcode with the approximated distribution above the topcode. To do this, we first a construct a kernel-smoothed CDF using the IPUMS data below the topcode. We then join the below-topcode CDF with the above-topcode CDF from the generalized Pareto distribution. To avoid any kinks around the join point we first adjust the above-topcode CDF such that it matches the CDF at the topcode for the below-topcode. We use numerical differentiation of this CDF to derive the full distribution for PDF adjusting for topcoding. To further avoid any kinks around the topcode, we cut incomes within

⁴⁴Since we are only able to define urban cores for the set of 27 CBSAs with sufficiently small PUMAs in 1990 and 2014, we estimate α_{tsn} only for the portion of state s that is covered by a CBSA in that sample.

⁴⁵We add the additional restriction that at least 1.5% of the total income distribution falls between $x_{m_{tsn}}$ and $x_{m_{tsn}}$ to ensure we have a sufficient data to estimate the shape parameter. If less than 1.5% of the total income distribution falls between those two points we lower the percentile cutoff by 1% percentage point until that condition is met.

⁴⁶The *gpinter* package approximates the income distribution using a set of income percentiles and the average income between each percentile. For each state, area, and period we use the same set for the first 6 percentiles: [10,30,45,60,75,85]. Then based on where the topcode falls for that particular distribution we allow the set of top percentiles to vary. If the topcode percentile p_t falls between the 85th and 92nd percentile, we include no additional moments between the 85th and p_t . If p_t falls between the 92nd and 93rd percentile, our top two percentiles are $[85 + \frac{p_t - 85}{2}, p_t]$. If p_t falls between 93rd and 96th percentile are top 3 percentiles are $[85 + \frac{(p_t - 85)}{3}, 85 + \frac{2(p_t - 85)}{3}, p_t]$. If p_t falls above the 9th percentile the top 4 percentiles are $[85 + \frac{(p_t - 85)}{4}, 85 + \frac{2(p_t - 85)}{4}, 85 + \frac{3(p_t - 85)}{4}, p_t]$.

⁴⁷The generalized pareto methodology requires an unbiased estimate of average income for some top quantile of income. We use our estimates of $\widehat{\alpha}_{tsn}$ from the simple Pareto distribution to approximate the average income above the topcode.

\$1,500 of the topcode and interpolate through the PDF. Using the total population in area n , state s , and period t we use this smoothed PDF to get a population estimate at each \$5,000 interval. Finally, we can aggregate across states to get the urban, suburban, and total distribution for each of the 27 CBSAs in our calibration sample in 1990 and 2014 and across samples to get the urban, suburban, and total distribution for our pooled “representative city” sample.

Appendix C.1.2 Smartphone Movement Data

The smartphone movement data is from October 2016 to August 2018. Our data provider aggregates data from multiple apps’ location services.⁴⁸ Each visit comes from raw movement data intersected with a basemap of polygons (usually buildings). Each visit receives a unique location, device, and time stamp.

We define the permanent home location of each device as in Couture et al. (Work in Progress), using 90 billion visits to residential establishments. We first identify a individual’s weekly home location as the residential location where it spends most night hours, conditional on visiting that location at least three different nights that week. We then assign a permanent home location to any device that has the same weekly home location for three out of four consecutive weeks. We are able to identify permanent homes for 87 million individuals between 2016 and 2018. We refer to this location as the person’s home location.

We have 9.6 billion visits to commercial establishments in our sample. Of these, our amenity demand estimation and method of moments use 2.3 billion that are to non-tradable amenities, defined as restaurants, gyms, movie theaters, and outdoor amenities (we exclude all retail locations). To identify visits starting from home, we use the time stamp and duration of each visit. We define a trip as from home if the previous visit was to home and ended less than 60 minutes earlier. That procedure identifies 220 million trips to non-tradable services that start from home.⁴⁹ Finally, for our quality estimation, we restrict the sample to 600 million visits to chain restaurants, 60 million of which start from home. We refer to Couture et al. (Work in Progress) for additional details on that data.

Table C.5 shows the number of establishment in the smartphone data basemap for the ten largest restaurant chains, compared with recent estimates of the actual number that we found online. This comparison shows that the smartphone basemap is nearly complete, with one exception, Starbucks, where almost half of the establishments are missing from the smartphone basemap.

⁴⁸Athey et al. (2018) and Chen and Rohla (2018) use similar smartphone data from a different provider. We refer to Couture et al. (Work in Progress) for evidence that the spatial distribution of smartphone devices provides a balanced representation of the U.S. population along a number of dimensions (CBSA, income, race, education); the distance traveled to different destinations implied by the smartphone data resembles that from the NHTS travel survey; and the mapping of commercial establishments visited by smartphone users to the business registry is relatively complete.

⁴⁹We do not observe all travel by individuals, so visit duration is a lower bound and missing in some cases. This explains why we are only able to ascertain 10 percent of trips as starting from home, whereas for instance about 30 percent of trips to restaurants in the NHTS start from home.

Table C.5: Ten Largest Restaurant Chains in NHTS vs Smartphone Data

Chain	NETS 2012 Rank	Smartphone 2016 Rank	NETS 2012 Count	Smartphone 2016 Count	Most Recent Actual Count
Subway	1	1	10,946	25,889	24,000+
McDonalds	2	2	9,889	14,914	14,000+
Starbucks	3	3	6,581	7,636	14,000+
Pizza Hut	4	6	5,754	6,695	7500+
Burger King	5	5	5,660	7,011	6500+
Wendys	6	8	4,127	5,683	5000+
Dunkin Donuts	7	4	4,030	7,418	8500+
KFC	8	14	3,997	3,157	4000+
Taco Bell	9	7	3,544	6,102	6000+
Dairy Queen	10	10	3,380	4,199	3500+

Notes: The data source from the most recent actual count obtained on 19 December 2018 from the following websites:

Subway: <https://www.subway.com/en-US/exploreourworld>

McDonald: <https://news.mcdonalds.com/our-company/restaurant-map>

Starbucks: <https://www.loxcel.com/sbux-faq.html>

Pizza Hut: <https://locations.pizzahut.com/>

Burger King: <https://locations.bk.com/index.html>

Wendys: <https://locations.wendys.com/united-states>

Dunkin Donuts: <https://www.dunkinonuts.com/en/about/about-us>

KFC <http://www.yum.com/company/our-brands/kfc/>

Taco Bell: <http://www.yum.com/company/our-brands/taco-bell/>

Dairy Queen: <https://www.qsrmagazine.com/content/23-biggest-fast-food-chains-america>

Appendix C.1.3 NETS Data

The 2012 National Establishment Time-Series (NETS) Database includes 52.4 million establishments with time-series information about their location, industries, performance and headquarters from 1990-2012. The NETS dataset comes from annual snapshots of U.S. establishments by Duns and Bradstreet (D&B). D&B collects information on each establishment through multiple sources such as phone surveys, Yellow Pages, credit inquiries, business registrations, public records, media, etc. Walls & Associates converts D&B's yearly data into the NETS time-series. The NETS data records the exact address for about 75 percent of establishments. In the remaining cases, we observe the establishments zip code and assign it's location to the zip code centroid.

Neumark et al. (2007) assess the NETS reliability by comparing it to other establishment datasets (i.e., QCEW, CES, SOB and BED data). Their conclusions support our use of the NETS data to compute a long 12-year difference from 2000 to 2012. They report that NETS has better coverage than other data sources for very small establishments (1-4 persons), which is often the size of consumption amenity establishments.

Table C.5 suggests that the NETS database is less complete than the smarphone basemap, but some of this difference is due to the earlier count. The NETS contains a majority of establishments for nine of the ten largest chains, with the exceptions of Subway where the NETS misses more than half the actual number of establishments. We further assess the precision of the NETS by considering aggregate growth of chain establishments. For instance, Chipotle had nearly 100 stores in 2000 and grew to about 1000 stores in 2010. The NETS reports 21 Chipotle stores in 2000 and around 840 in 2012. Together, these numbers show that the NETS data captures general growth patterns, but we struggle to identify all chains due to merging on inconsistent establishment names and lags in D&B recording new locations.

Appendix C.1.4 Zillow House Price Indexes

Our main house price index comes from Zillow.com.⁵⁰ Our 2 bedroom index is the Zillow House Value Index (ZHVI) for all two-bedroom homes (i.e., single family, condominium, and cooperative), which is available monthly for 8,030 zip codes in 1996, 8,031 zip codes in 2000, 8,575 zip codes in 2012, and 8,898 zip codes in 2016. In robustness checks, we use the per square foot Zillow House Value Index for All Homes, which is available monthly for 14,417 zip codes in 1996, 14,421 zip codes in 2000, and 15,500 zip codes in 2014. For each zip code in the Zillow data, we compute a yearly index by averaging over all months of the year. We map zip codes to tracts with a crosswalk from HUD. We compute the tract-level index as the weighted average of the home value index across all zip codes overlapping with the tract, using as weights the share of residential address in the tract falling into each zip code. For tracts falling partly into missing zip codes, we normalize the residential share in zip codes with available data to one. The final data set contains the 2 bedroom

⁵⁰We collected the data in February 2019. The index and methodology are available at: <http://www.zillow.com/research/data/>.

index for around 35,000 tracts in each year, and the all home index for around 53,000 tracts in each year.

Appendix C.1.5 National Household Transportation Survey (NHTS)

The National Household Travel Survey (NHTS) conducted by the Federal Highway Administration (and local partners) provides travel diary data on daily trips taken in a 24-hour period for each individual in participating households. We use the 2009 NHTS survey. Each trip has a WHYTO (trip purpose) code that we match to work purposes to compute commute cost τ_D and τ_S . Work trip purposes are:

1. Work (WHYTO 10)
2. Go to work (WHYTO 11)
3. Return to work (WHYTO 12)
4. Attend business meeting/trip (WHYTO 13)
5. Other work related (WHYTO 14)

We use weights at the person level to compute population estimates of mean trip shares.

Appendix C.1.6 Subsidized and Public Housing

We use tract-level data from HUD on the total number of households living in federal subsidized or public housing in 2000 and 2014. HUD reports the total number of available units by housing program. They also report the share of households in each tract living in subsidized or public housing across different income brackets. We standardized income brackets between 2000 and 2014 by assuming that households are uniformly distributed within a bounded bracket. For any tracts with missing data or no units reported, we assume that no households within that tract were living in public or subsidized housing. We observe 57,502 tracts in 2000 and 42,467 tracts in 2014 with subsidized or public housing.

Appendix C.2 Variable Definitions

This subsection details the computation of variables used in section 3 onwards in the paper.

Appendix C.2.1 CBSA Level Wage Bartik shock

We use a Bartik wage shock to predict CBSA-wide average income growth between 1990-2014 and 2000-2014. We determine industry growth using 3-digit Census industry codes in 1990. The Census Bureau provides crosswalks between 2000, 2012, and 1990 industry codes. Examples of 3-digit industry categories includes "Aluminum production and processing", "Shoe Stores", "Retail Florists", and "Real Estate".

To calculate national wage growth for each industry between 1990-2014 or 2000-2014, we use person-level IPUMS data in 1990, 2000, and 2014. We keep the sample of people between 21 and 55 years who work at least 35 hours a week in a non-farm profession. We use annual pre-tax wage and salary income for individual earners. As is standard we compute a CBSA-leave out growth for each CBSA.

For both the Bartik shock from 1990-2014 and 2000-2014, we fix the share of people working in each 3-digit census industry for each CBSA in 1990. As in Diamond (2016), we compute wage growth in each industry as the (leave out) difference in average log wage across years. Our Bartik income shock is then wage growth weighted by initial 1990 industry shares in each CBSA. For our robustness specifications, we compute Bartik shocks leaving out two major industry categories: Finance, Real Estate and Insurance (1990 industry codes 700-712), and Technology.⁵¹ We also compute Bartik shocks leaving out the top quartile of most urbanized industries. Table C.7 shows the 10 most and 10 least urbanized industries in 1990.

Appendix C.2.2 Median Income within Census Table Brackets

The U-shape plot in Figure 1 shows median income within each family income brackets from the NHGIS Census tables. To find the median income within each census bracket, we use the distribution of family income within the 100 largest CBSAs in the IPUMS microdata in the corresponding year. To adjust for topcoding in IPUMS, we estimate the shape of the IPUMS income distribution above the 95th percentile assuming a Pareto distribution.

The estimation of ρ also requires median income within each census bracket. In this case, however, the estimation requires constant bracket over time. To do this, we assume that households are uniformly distributed within each bracket, except for the top bracket. We can then map each CPI-adjusted census brackets in 1990 and 2000 onto 2014 bracket definitions, setting median income w as the mid-point of these constant brackets. For the top bracket (above \$140,600 in 1999 dollars), we determine median income using 2000 IPUMS microdata.

Appendix C.2.3 Yearly User Cost of Housing ($p_{nj,c}^h$).

Computing $p_{nj,c}^h$ We first compute a population weighted-median house price over all tracts in a given area quality pair in a given CBSA. To obtain $p_{nj,c}^h$ that we use in estimation and calibration, we multiply this median house value by a user cost of housing equal to 5.0 percent of house value in 1996, 4.7 percent in 2000 and 4.6 percent in 2014. These rent-price ratios come from the Lincoln Institute of Land Policy.⁵²

⁵¹181 = Pharmaceuticals; 342 = Electronic component and product manufacturing ; 352 = Aircraft and Parts ; 362 = Aerospace products and parts manufacturing ; 891 = Scientific research and development services ; 732 = Computer systems design and related services + Software Publishing + Data processing, hosting, and related services; 882 = Architectural, engineering, and related services.

⁵²Data collected in October 2018 from <https://datatoolkits.lincolninst.edu/subcenters/land-values/rent-price-ratio.asp>.

Property Taxes as a Share of $p_{nj,c}^h$ Using CPI-adjusted tract-level ACS and Census estimates of the median property taxes for owner-occupied units, we find the population-weighted median amount paid in property taxes in 1990, 2000, and 2014 for each area quality pair. We then divide this amount by $p_{nj,c}^h$.

Appendix C.2.4 Tract Level Quality Index.

Estimating Chain Quality We define quality for the 100 largest restaurant chains, with the most establishments in the smartphone data basemap. We index block groups by i , venues by j , and chains by c . We denote by N_{ic} the total number of visits by individuals living in block i that start from home and end in venues in chain c within its CBSA. Restricting our sample of chain visits to those that start from a person’s home isolates the choice of visiting a chain from other considerations of travelers (e.g., eating during lunch at work).

We further control for proximity to venues within that chain to isolate chains that high income people like from chains that simply co-locate with them. Our main specification has two controls for proximity of block i to venues in chain c : first the normalized straightline distance between the centroid of block i and the closest venue j in chain c , denoted by $dist_{ic(closest)}$, and second the normalized number of establishments in chain c within 5 miles of block i , denoted by $num5mil_{ic}$.⁵³ Our estimation sample consists of 2.3 million block*chain pairs with at least one within-CBSA visit from home. In a first step, we purge the number of visits from the impact of proximity to chains by running:

$$\ln N_{ic} = \beta_1 + \beta_2 \ln(dist_{ic(closest)}) + \beta_3 \ln(num5mil_{ic}) + \epsilon_{ic}.$$

We then compute a number of visits purged of proximity as:

$$\widehat{N}_{ic} = \exp \left(\ln N_{ic} - \widehat{\beta}_2 \ln(dist_{ic(closest)}) - \widehat{\beta}_3 \ln(num5mil_{ic}) \right)$$

In the next step, we compute the relative propensity of high income individuals to visit each chain, relative to the average device. We assign income at the block group level, and define as high income block groups that had median income of \$100,000 per year in 1999 dollars in the latest ACS (2014). The share of visits to chain c out of total visits to the 100 largest chains, among individuals living in high income block groups, is:

$$S_c^{High} = \frac{\sum_{i \in I_c} \widehat{N}_{ic}^{High}}{\sum_{c=1}^{100} \sum_{i \in I_c} \widehat{N}_{ic}^{High}},$$

where I_c is the set of block groups with a positive number of visits to chain c . We can then define the quality of chain c as the propensity of individuals in high income block groups to visit chain c

⁵³We normalize $dist_{ic(closest)}$ to equal 1 at the median distance of the closest venue for that chain, computed across all blocks with at least one visit to that chain. The variable $dist_{ic(closest)}$ is then in multiples of that median distance. We do this to ensure that our distance-adjusted number of visits remains unchanged for a block at median distance from chain c .

relative to that of individuals in the average block:

$$Quality_c = \frac{S_c^{High}}{S_c},$$

where $Quality_c = 1$ means that high income individuals are as likely to visit chain c as the average device, controlling for differences in proximity to venues in chains c .

We perform a number of robustness checks. First, we note that excluding block*chain pairs with zero visits from home is likely to bias our quality index against chains that locate far from high income residents. We experiment with including all block*chain pairs with zero visits in our regression and index computation, and obtain an index with a correlation of 0.94 with our preferred index.⁵⁴ We also experiment with different income cut-off and find that an index defining high income blocks as having median income above \$75,000 has a correlation of 0.93 with our preferred index. Finally, we experiment with adding controls for number of chains farther away than 5 miles, and for demographic similarity between block i and the block in which the closest venue in chain c is located (median income difference, age difference, share college difference, EDD measure of racial dissimilarity in Davis et al. Forthcoming). The correlation of these indices with our preferred chain quality index is above 0.98.

From Chain Quality to Tract Quality In the NETS data, we can find all of the 100 largest chains in the smartphone data in 2012, accounting for 64,000 establishments, and 96 chains in 2000, accounting for 49,000 establishments.⁵⁵ We compute quality at the tract level as the average quality of all chains within the tract. If a tract contains fewer than 3 chains, we take the average over all tracts with centroid within 0.25 mile from the tract, and so on in further 0.25 mile increment until there are at least 3 chains. We set a limit of 1.5 miles in urban areas, and 3 miles in suburban areas, below which we set quality to missing if there are still fewer than 3 chains within that limit. This procedure generates 4 percent missing tracts in urban areas, and 15 percent in suburban areas.⁵⁶

Appendix C.3 Downtown Census Tracts for Some CBSAs

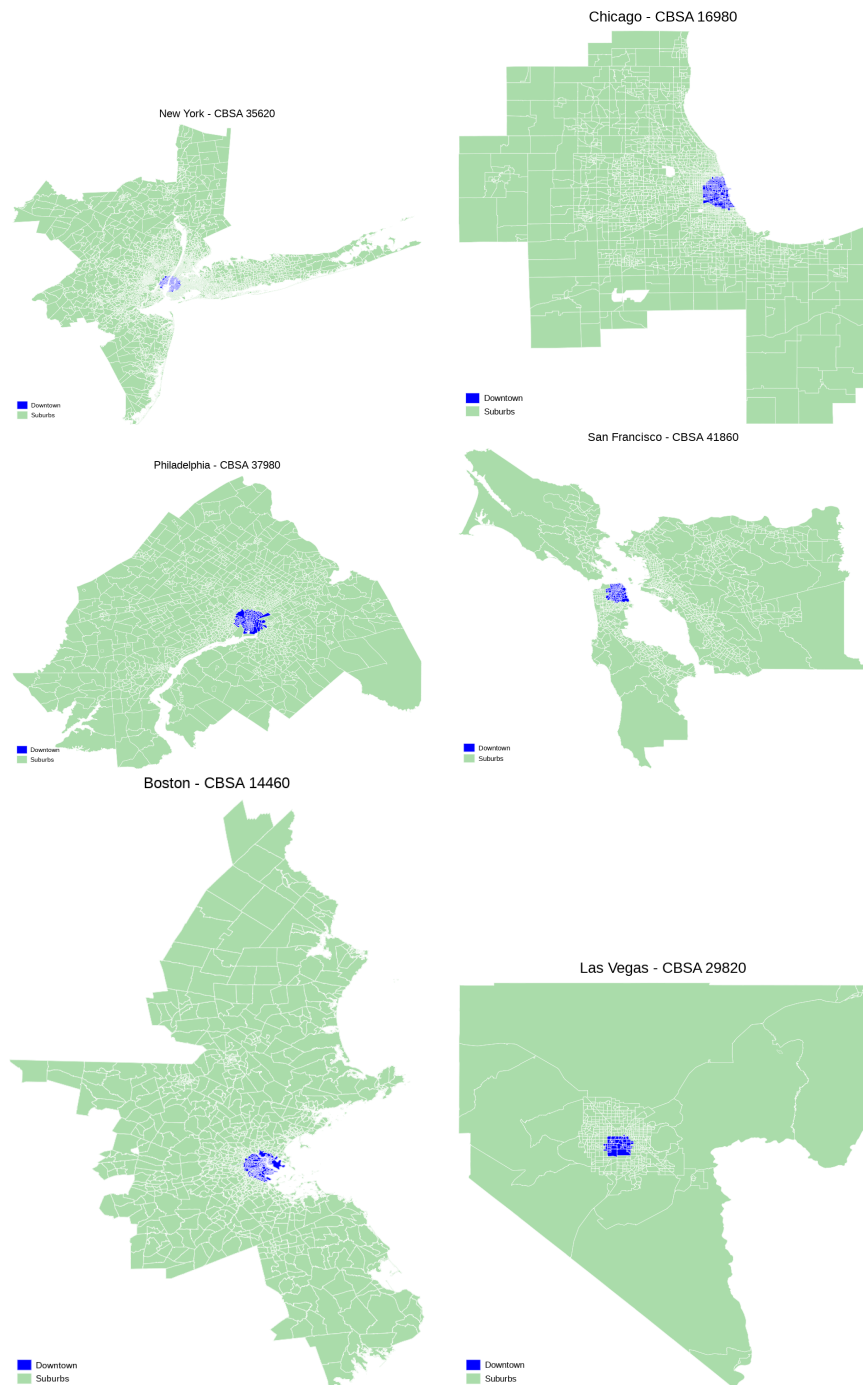
Figure C.3 shows the downtown and suburban tracts for the CBSAs of New York, Chicago, Philadelphia, San Francisco, Boston, and Las Vegas. Figure C.4 shows income growth in downtown and selected suburban tracts within the central county of each of these CBSAs.

⁵⁴In that case, $N_{ic} = 0$ gets adjusted upward if the closest venue to block i is farther than median distance, and therefore included as a positive number of visits in the index computation, possibly creating the opposite bias as in our preferred specification. We use the invert hyperbolic sine transform to allow for log of zeros.

⁵⁵The earliest NETS data is in 1992, but we cannot reliably define tract quality so far back in the past, because too many of the largest chains in our 2016-2018 smartphone data only experienced national growth after 1992.

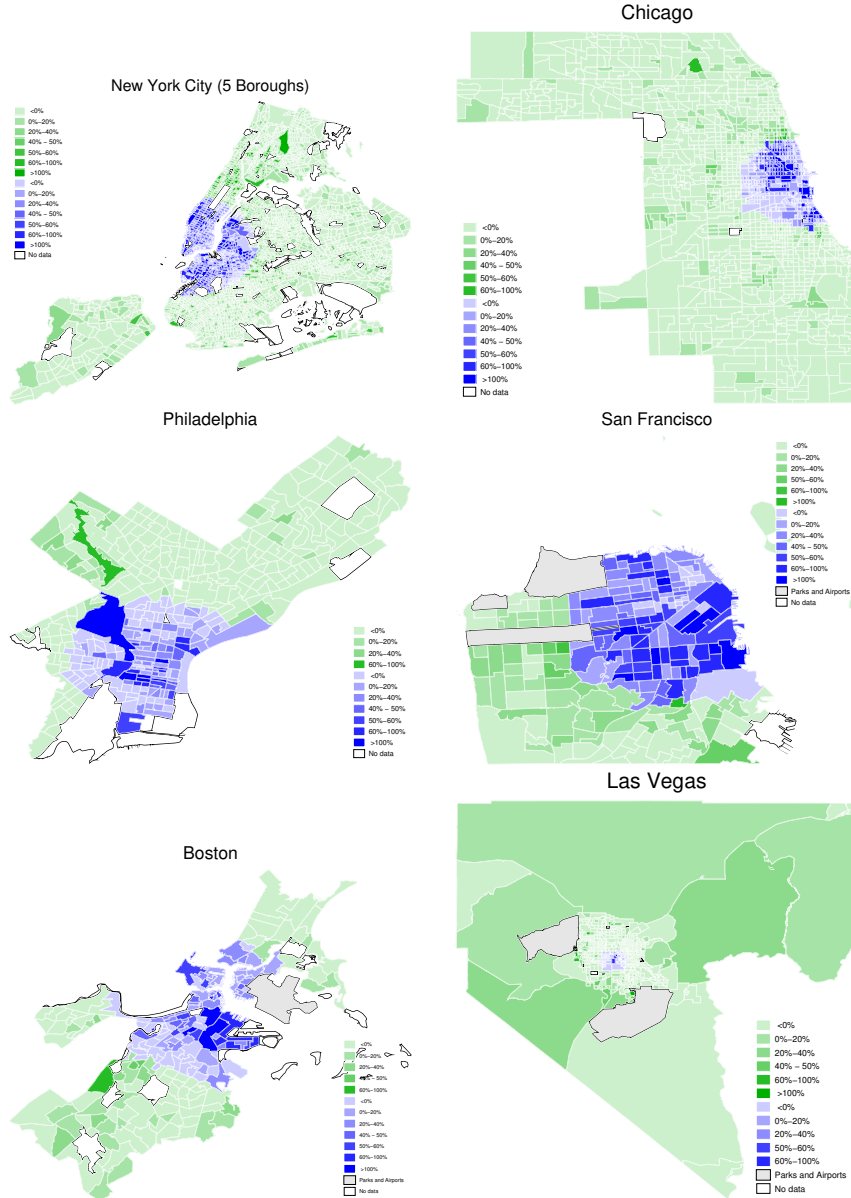
⁵⁶For urban tract, there are at least three chains within tract for 15 percent of tracts, within 0.5 miles for 29 percent of tracts, and within 1 mile for 73 percent of tracts. For suburban tracts, there are at least three chains within tracts for 20 percent of tracts, within 0.5 miles for 25 percent of tracts, within 1 mile for 55 percent of tracts, and within 2 miles for 86 percent of tracts.

Figure C.3: Downtown and Suburban Tracts in Selected CBSAs.



Note: Downtown tracts in dark blue consists of all tracts closest to the city center and accounting for 10% of total CBSA population in 2000.

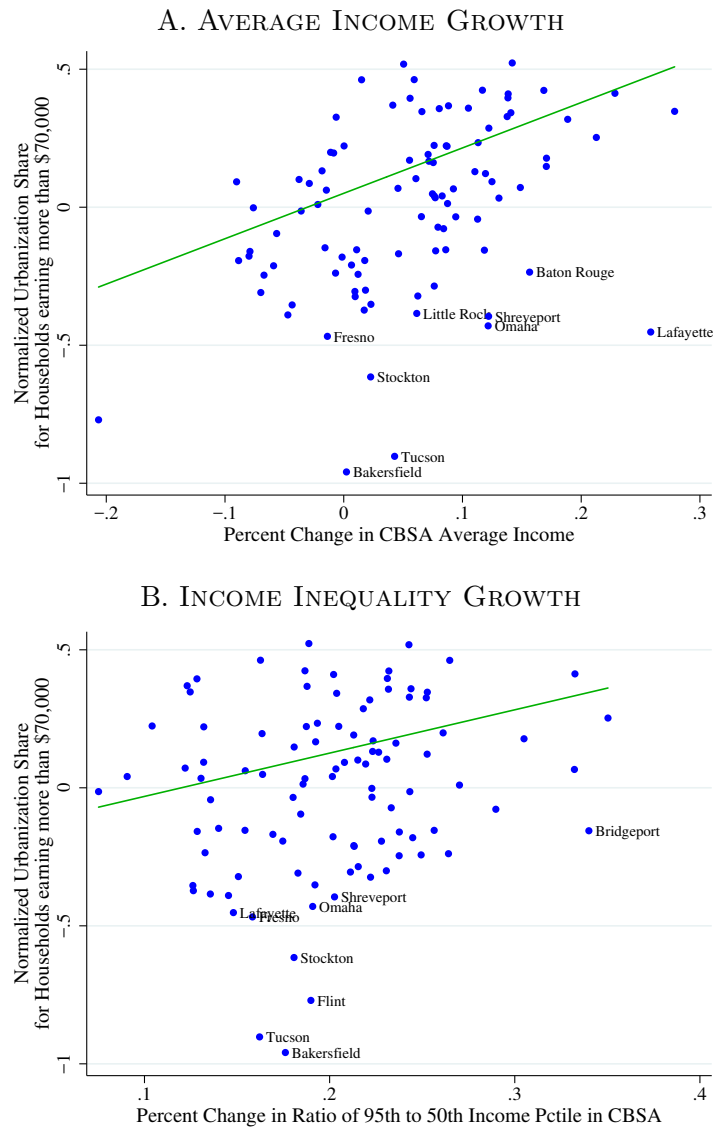
Figure C.4: Income Growth in Tracts in Central County of Selected CBSA



Note: Each map shows the central county of a given CBSA, except for New York which shows the five counties (boroughs) of New York City. Downtown tracts in blue consist of all tracts closest to the city center and accounting for 10% of total CBSA population in 2000. The shading of each tract shows its percent growth in median household income between 1990 and 2014.

Appendix C.4 Alternative Representation of Changing Sorting Patterns

Figure C.5: Change in the Propensity of Richer Households to Live Downtown and Income Growth Across CBSAs Between 1990 and 2014



Note: These figures show how changes in the location choices of high-income households correlate with income growth in each of the 100 largest CBSAs. The y-axis of each plot shows change in the share of individuals earning \$70,000 or more residing downtown relative to the average individual between 1990 and 2014. In Panel a, these location changes are plotted against the average CBSA real household income growth between 1990 and 2014 on the x-axis. The green line through the scatterplot depicts weighted linear fit (where the weights are the CBSA 1990 population) with a slope coefficient of 1.64 and standard error of 0.32. In Panel b, the location changes are plotted against the percent growth in the ratio between the 95th and 50th percentiles of the CBSA's income distribution over the same period. The green line through the scatterplot depicts weighted linear fit (where the weights are the CBSA 1990 population) with a slope coefficient of 1.57 and standard error of 0.56.

Table C.6: Robustness exercise for ρ estimation.

	2000-2014 (1)	Zillow All Price (2)	Census Price (3)
$\hat{\rho}$	3.10 (1.01)	1.94 (0.56)	2.67 (1.00)
Instrument	Base	Base	Base
KP F-Stat	8.4	5.3	3.7
Obs	5,901	6,632	7,031

Notes: This table shows estimates from equation (23). Data from 100 largest CBSAs, from 2000 and 2014 in column 1 and from 1990 and 2014 in column 2 and 3, neighborhood quality defined from education mix of residents. Each observation is weighted by the number of households in the income bracket with the fewest households amongst the four brackets in each independent variable. Standard errors clustered at the CBSA-quality level are in parentheses. KP F-Stat = Kleinberger-Papp Wald F statistic.

Appendix C.5 Robustness of Estimation of ρ

Our preferred estimate of ρ from equation (23) is shown in column 2 of Table 1. Here, we show variants of this estimation in Table C.6. In column 1, we change the time period from 1990-2014 to 2000-2014. In column 2 and 3, we change the house price index from Zillow 2 Bedroom to Zillow All Home in column 2, and to the Census median house price in column 3. These IV estimates are noisier than our base estimate, but they range from 1.94 to 3.10, which is within two standard deviations from our preferred estimate of $\rho = 3.0$.

We also explored the robustness of our estimate to changes in our high quality cut-off from at least 40 percent college share, to at least 30, 50, or 60 percent college share. Estimates are noisier for the highest cut-offs which contain a very small share of high quality tracts, but IV estimates remain between 2.10 and 4.52.

Finally, Table C.7 provides additional detail on the robustness exercise in the main text where we drop the most urbanized industries from our Bartik instrument. The table shows the 10 most urbanized and 10 least urbanized industries, along with the share of urban workers in that industry. The table highlights that even for the most urbanized industry (Museum, Art Galleries, Historical Sites, and Similar Institutions) the share of urban workers is only 24 percent, so that most of the Bartik variation comes from the suburbs. This is because our urban areas, by construction, are small relative to the suburbs.

In section 3.1, we define two separate measures of neighborhood quality. First, we define high quality neighborhoods as those that contain 40 percent of residents with at least a bachelor's degree. In the main text, we show our estimation and counterfactual results using this baseline college share definition. Second, we define high quality neighborhoods as those that have a chain

Table C.7: Most and Least Urbanized Industries

Code	Industry	Urban Share
872	Museums, art galleries, historical sites, and similar institutions	24.8%
762	Traveler accommodation	20.6%
151	Cut and sew apparel manufacturing	20.5%
800	Motion pictures and video industries	20.2%
750	Car Washes	19.5%
900	Executive offices and legislative bodies	19.2%
761	Private households	18.9%
721	Advertising and related services	18.4%
951	U. S. Coast Guard	18.4%
542	Apparel, fabrics, and notions wholesalers	17.6%
...
352	Aircraft and Parts	4.0%
622	Other motor vehicle dealers	3.8%
311	Agricultural implement manufacturing	3.6%
950	U. S. Marines	3.4%
561	Farm supplies wholesalers	3.2%
41	Coal Mining	2.8%
362	Guided Missles, Space Vehicles, and Parts	2.7%
821	Office of chiropractors	2.5%
590	Miscellaneous retail stores	2.3%
11	Animal production	1.2%

Notes: This table shows the 3-digit industries with the highest share of workers who live in urban areas in row 1 to 10, and industries with the lowest share in row 11 to 20. IPUMS data from the 27 CBSAs with constant geography urban area in 1990 and 2014. These urban areas contain 10 percent of each CBSA's population in 2000.

restaurant index greater than 1.1. Here we show that relative to using the college share quality definition, the restaurant chain quality definition delivers somewhat lower ρ estimates.

Table C.8: ρ Restaurant Cutoff Robustness

	1.0		1.1		1.2		1.3	
	(1) OLS	(2) IV	(3) OLS	(4) IV	(5) OLS	(6) IV	(7) OLS	(8) IV
ρ	1.73 (0.16)	1.21 (0.64)	1.64 (0.23)	1.62 (1.41)	1.78 (0.24)	2.64 (2.37)	1.83 (0.26)	2.55 (2.20)
Instrument	None	Base	None	Base	None	Base	None	Base
R ²	0.25		0.19		0.18		0.20	
KP F-stat		5.52		3.20		2.43		3.09
Obs	5284	5284	4782	4782	4383	4383	4085	4085

Notes: This table shows estimates from equation (23). Data from 100 largest CBSAs in 1990 and 2014, neighborhood quality defined based on chain restaurant quality. Each observation is weighted by the number of households in the income bracket with the fewest households amongst the four brackets in each independent variable. Standard errors clustered at the CBSA-quality level are in parentheses. KP F-Stat = Kleinberger-Papp Wald F statistic. Columns 1-2 define high quality tracts with an average restaurant index of at least 1.0.

Appendix D Quantification Appendix

This appendix provides more details on how we select the parameters used in the baseline calibration.

Appendix D.1 Estimation and Parametrization of Demand Parameters (α , δ , σ , and γ)

We first discuss the estimation of the demand system for consumption of non-traded amenities. Specifically, we focus on estimating δ and σ (defined in Equation (B.10)) using a model-implied gravity equation. We then parameterize α , the share of net disposable income spent on urban amenities using expenditure data (see Equation (1)). Finally, we discuss our parametrizations of γ , the Fréchet shape parameter that governs love of variety for neighborhoods of a given type (see Equation (2)). Throughout, we define residential amenities as non-tradable services such as restaurants, bars, entertainment venues (movie theater, shows, etc), gyms, and other personal services. When thinking of residential amenities, we exclude retail consumption at apparel, grocery, and other merchandise stores. Non-tradable services like restaurants and entertainment venues most closely match our model’s neighborhood amenities that are luxurious, endogenous, locally-provided, and subject to strong economies of density.

The model delivers the following gravity equation for amenity demand:

$$\ln \left(\frac{a_{rr'}}{a_{rr}} \right) = \ln \left(\frac{\beta_{rr'}^q}{\beta_{rr}^q} \right)^{\beta_{j(r) \neq j(r')}} - \sigma \delta \ln \left(\frac{d_{rr'}}{d_{rr}} \right) - \sigma \ln \left(\frac{p_{r'}^a}{p_r^a} \right)^{\theta_r + \theta_{r'}}. \quad (\text{D.27})$$

The first term captures the possibility that people place a different value on consuming amenities of a quality type other than that of their home neighborhood. We proxy this with a dummy variable $\beta_{j(r) \neq j(r')}$ equal to 1 when the home neighborhood r is of a different quality type than the destination neighborhood r' . The second term captures the travel distance required to access amenities in neighborhood r' relative to the travel distance required to access amenities within the home neighborhood r . The third term captures relative amenity prices in neighborhood r' and r . We control for this term with an origin r and a destination r' fixed-effect, θ_r and $\theta_{r'}$. Importantly, these fixed-effects can absorb any unobserved tract characteristics. We then obtain the following estimating equation:

$$\ln \left(\frac{a_{rr'}}{a_{rr}} \right) = \beta_{j(r) \neq j(r')} - \sigma \delta \ln \left(\frac{d_{rr'}}{d_{rr}} \right) + \theta_r + \theta_{r'} + \epsilon_{rr'}. \quad (\text{D.28})$$

Estimating equation (D.28) requires information on the origin and destination of a large number of trips to consume amenities, which is not available in conventional travel surveys. To circumvent this issue, we again make use of the new smartphone movement data. It allows us to identify 2.3 billion trips to commercial establishments that we classify as non-tradable services, namely restaurants,

gyms, theaters, and outside amenities, from 87 million devices for which we can identify a permanent home location. In order to isolate the choice of consuming amenities from other considerations of travelers, we study the robustness of our estimates to restricting the sample to only trips starting from home, to trips starting from home and coming immediately back home, or to trips that take place on weekends. We again define neighborhoods as census tracts, so $a_{rr'}$ is the number of trips by people living in tract r to non-tradable service establishments located in tract r' . We define $d_{rr'}$ as the haversine distance from the centroid of tract r to that of tract r' and δ_{rr} as half the radius of the home tract. Each observation in our regression is a tract pair rr' and we limit the choice set of each individual to tracts available within their CBSA. Note that $\delta\sigma$ is large if people make few trips far from home, either because the cost of distance δ is large or because amenities are highly substitutable (i.e., σ is large).

Table D.9 shows the estimation results. The coefficients $\delta\sigma$ are stable and remain within 1.17 and 1.57 across all specifications. Interestingly, our amenity trip gravity coefficients are similar, albeit somewhat larger, to those from the trade literature, which center around 1 (Disdier and Head, 2008), and resemble the estimate of 1.29 for regional trade in the U.S. from Monte et al. (2018).⁵⁷ The coefficients on $\beta_{j(r)\neq j(r')}$ are consistently negative and significant, indicating a distaste for visiting neighborhoods with quality other than one’s home neighborhood, and providing some evidence that our quality definition captures relevant features of household’s preference for amenities. In fact, in our data, high quality tract residents take over 80 percent of their amenity trips to other high quality tracts, and low quality tract residents also take over 80 percent of their amenity trips to other low quality tracts. Our $\delta\sigma$ estimates are robust to adding additional controls for tract pair characteristics, such as an index of racial dissimilarity and median age difference. We also obtain similar estimates using the restaurant chain quality definition instead of the college share definition, as shown in Table D.10.

The above gravity equation estimates $\sigma\delta$. However, for our calibration, we need estimates of σ and δ separately. We are not aware of existing estimates of δ that map into our model’s parameter. As discussed below, we find a δ around 0.2 using data from Couture (2016). Given our estimate of $\sigma\delta = 1.3$ from Table D.9, we recover $\sigma = 6.5$, which reassuringly stands midway in the range of values from the existing literature. Atkin et al. (2018) find an elasticity of substitution of 3.9 for retail stores in Mexico, Einav et al. (2019) find 6.1 for offline stores in the U.S., Su (2018a) and Couture (2016) find 7.5 and 8.8 respectively for restaurants in the U.S. So we pick $\delta = 0.2$ and $\sigma = 6.5$ as our baseline parameters and explore robustness over the range of values above. Finally, because the land area of downtown and the suburbs change endogenously between equilibria in the model, the representative distance between two neighborhoods also changes. We make the

⁵⁷There is limited evidence on the strength of gravity in travel to consumption amenities. Agarwal et al. (2019) find much smaller distance elasticities of around -0.4 for different consumption sectors using credit card transaction data at the census place level. Davis et al. (Forthcoming) use Yelp restaurant reviews in New York City to find review elasticity between -1.1 to -1.5 with respect to travel time from home, and Athey et al. (2018) find a distance elasticity of -1.4 using smartphone visits to restaurants in San Francisco. Our estimates here confirm the values in the latter two papers, using a much larger sample in individual, product, and geographic space, and solving an important identification problem by selecting trips whose sole purpose is amenity consumption.

Table D.9: Estimation of gravity parameter $\sigma\delta$

	All (1)	Home (2)	Weekend (3)	Home-Home (4)
$\hat{\delta}\sigma$	1.57 (0.00)	1.42 (0.00)	1.20 (0.00)	1.18 (0.00)
$\beta_{j(r)\neq j(r')}$	-0.14 (0.00)	-0.12 (0.00)	-0.10 (0.00)	-0.09 (0.00)
R^2	0.91	0.87	0.88	0.85
Obs	22,791,347	6,403,153	11,924,874	3,050,752

Notes: This table shows estimates from equation (D.28). From smartphone data on trips to non-tradable services in 100 largest CBSAs in 2016-2018, and neighborhood quality defined based on education mix of residents. All: sample of all trips, Home: trips starting from home, Weekend: trips taken on weekend, Home-Home: trips starting from home and returning directly back home. See main text for a description of the regression.

Table D.10: Gravity Parameter $\sigma\delta$ Restaurant Robustness

	All (1)	Home (2)	Weekend (3)	Home-Home (4)
$\hat{\delta}\sigma$	1.56 (0.00)	1.40 (0.00)	1.18 (0.00)	1.17 (0.00)
$\beta_{j(r)\neq j(r')}$	-0.04 (0.00)	-0.03 (0.00)	-0.03 (0.00)	-0.03 (0.00)
R^2	0.91	0.87	0.88	0.85
Obs	9,858,033	5,645,813	10,419,101	2,696,680

Notes: This table shows estimates from equation (D.28). From smartphone data on trips to non-tradable services in 100 largest CBSAs in 2016-2018, and neighborhood quality defined based on chain restaurant quality. All: sample of all trips, Home: trips starting from home, Weekend: trips taken on weekend, Home-Home: trips starting from home and returning directly back home. See main text for a description of the regression and Appendix C for data details.

geometric assumption that the representative distance d_{nn} changes with the square root of the area of n , K_n , while $d_{nn'}$ changes with the square root of $K_n + K_{n'}$.

We now parametrize α , the share of expenditures on local amenities such as restaurants, bars, entertainment venues, gym memberships, and other personal services, net of housing costs and transportation to work. In the 2013 Consumer Expenditure Survey (CEX), food away from home and entertainment fees and admission represent 6.2% of spending out of the average individual total expenditures. Given that housing is about 27% of total expenditures (including utilities) and transportation to work is about nine percent of total expenditures, restaurant and entertainment spending alone represent 10 percent of expenditure net of housing costs and transportation. Adding in other residential amenities such as bars, gym memberships, and other personal services yields roughly another few percentage points of expenditures net of housing and transportation. As a result, our base calibration uses $\alpha = 0.15$, and we investigate the robustness of our results to $\alpha \in [0.10, 0.30]$. The lower bound makes the narrow assumption that our residential amenities only include restaurants and entertainment. The upper bound allows for the fact that there are other luxury residential amenities (e.g., shopping experiences more broadly) that households are willing to pay for and that also evolve endogenously. As we show below, in the model, the higher the value of α , the larger the amplification in welfare differences between the rich and the poor due to the spatial sorting response following a rise in income inequality.

Finally, we parametrize γ , the elasticity of demand between neighborhoods. γ determines the size of gains from variety as the number of neighborhoods within an nj pair expands. Given the assumptions on idiosyncratic preference shocks, ρ must be lower than γ . This bounds γ from below. Existing research, on the other hand, suggests that there is less socio-economic diversity within census tracts than there is within retail establishments such as grocery stores and restaurants.⁵⁸ In the context of our model, this suggests that the substitution elasticity for residential amenities (σ) is an upper bound for γ . Given the estimation above, γ lies between 3.0 and 6.5. The lower the value of γ the larger the endogenous response of amenities to the changing income distribution. For our base assumption, we use a conservative value of $\gamma = 6.5$. As a robustness exercise, we present the sensitivity of our results to alternative parametrizations.

Appendix D.1.1 Calibrating δ

In this subsection, we discuss how we calibrate the parameter δ . Combining data on restaurant trips, prices, and expenditures with existing empirical estimates of value of travel time, Couture (2016) finds that a significant majority (59%) of trips to a restaurant from home take between 5 and 15 minutes, and that over this range of travel times, the total price of amenity rises by 27% due to travel costs. If we similarly calibrate δ such that tripling distance increases travel cost by

⁵⁸Handbury et al. (2015) find that Nielsen panelists who are from college- and non-college educated households are more likely to co-locate in grocery stores than in census tracts. This is consistent with Davis et al. (Forthcoming) who find a higher rate of racial segregation across residential neighborhoods than restaurants within NYC.

27% percent, we obtain:⁵⁹

$$\frac{d_{rr'}^\delta p^a}{d_{rr''}^\delta p^a} = \left(\frac{15}{5}\right)^\delta = 1.27 \quad (\text{D.29})$$

and recover $\delta = 0.22$.

Appendix D.2 Parametrization of Land Market Transmission Mechanism (ϵ_S and ϵ_D)

In the model, the area-specific elasticity of land supply ϵ_n is equivalent to an elasticity of housing supply. This elasticity determines the strength of an important welfare transmission mechanism through land markets. When housing supply is inelastic, an influx of rich households in high quality neighborhoods downtown raises rents for poor incumbent households in low quality neighborhoods. Saiz (2010) provides housing supply elasticity estimates ϵ_c for 95 large Metropolitan Statistical Areas, based on geographical constraints and housing regulations. We match 83 of these MSAs to our CBSA sample. Unfortunately, these are not estimated separately for downtown and suburban areas. To calibrate ϵ_D and ϵ_S , we posit that housing supply elasticities vary systematically, in equilibrium, with average household density ($density_c$), and estimate the following log-linear regression of ϵ_c on $density_c$:

$$\ln(\epsilon_c) = 1.97 - \frac{0.30}{(0.07)} \ln(density_c) + \xi_c^\epsilon, R^2 = 0.21 \quad (\text{D.30})$$

We rely on cross-CBSA variation to estimate this equation. We then define $\hat{\epsilon}_D$ and $\hat{\epsilon}_S$ as the fitted values from equation (D.30) computed at typical density of D and S neighborhoods in the 100 largest CBSAs. We find $\hat{\epsilon}_D = 0.60$ and $\hat{\epsilon}_S = 1.33$.⁶⁰ We use these values in our baseline calibration and test the sensitivity of our results to alternative parameter values.

Appendix D.3 Parametrization of Commuting Costs (τ_S and τ_D)

To estimate an area-specific commuting cost τ_n , we use data on trip time to work by car from the geo-coded 2009 National Household Travel Survey. Specifically, the average daily commute time for drivers living in the suburbs of the top 100 CBSAs is 64 minutes, while for those living downtown it is 47 minutes. We compute τ_n by assuming that each worker allocates 9 hours per day to working and commuting, and by valuing an hour of commuting at half of the hourly wage as recommended by Small et al. (2007). This implies a per labor hour commute cost of $\tau_n = 0.5 \times \text{CommuteTime}_n / 9$, or $\tau_D = 0.044$ and $\tau_S = 0.059$.

⁵⁹This result is not reported by Couture (2016), who uses a different parametrization of distance than that in our paper, but it can be computed with the data reported in that paper.

⁶⁰In our downtowns, the average CBSA population-weighted household density is 4,300 households per square mile, versus 300 in the suburbs. The highest density CBSA, New York, has 850 households per square mile, so the average density in D is out-of-sample. However, $\hat{\epsilon}_D = 0.60$ turns out to equal the elasticity of housing supply in Miami, which is the metropolitan area with the most inelastic housing supply in Saiz (2010).

Table D.11: Income and Homeownership Rates by Income Decile

Decile	Income (\$1,000s)			2000 Homeowner Share	
	1990	2014	% Growth	Downtown	Suburbs
1	28.3	28.0	-0.94	32%	49%
2	34.7	34.1	-1.95	35%	53%
3	41.4	40.7	-1.75	39%	57%
4	48.5	48.2	-0.57	43%	62%
5	56.2	56.7	0.94	48%	68%
6	64.9	66.7	2.80	51%	73%
7	75.3	79.0	4.89	55%	77%
8	89.0	96.0	7.86	60%	82%
9	110.7	123.6	11.63	65%	87%
10	168.6	198.5	17.73	71%	91%

Notes: This table shows the average income in 1990 and 2014 and 2000 homeownership rate of households by income decile in 2000, using data from IPUMS. See Appendix C for details on this data source.

Appendix D.4 Parameterization of Public Amenities and Homeownership

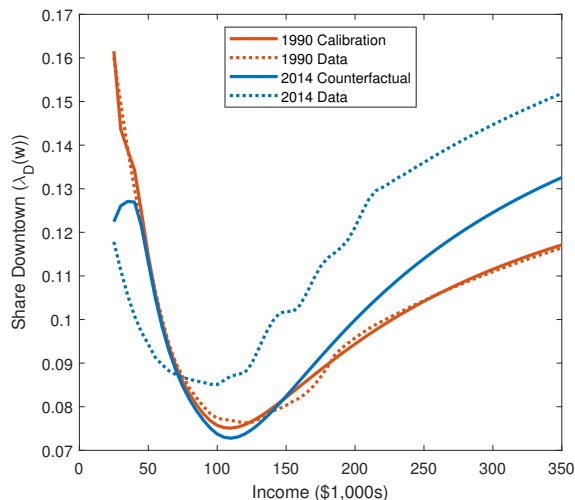
A household earning labor income w , receives a transfer of $\chi(w) = OS(w)\lambda_{1999,n_j}(w) \sum_{n_j} (p_{2014,n_j}^h - p_{1990,n_j}^h)$, where $OS(w)$ is the share of households with income w who reported owning homes in the 2000 IPUMS data (see table D.11). This allows us to forgo taking a stance on the initial level of $\chi(w)$ and instead only focus on the changes in $\chi(w)$ over time that results from house price growth due to the income inequality shock that we study.

Appendix E Counterfactual and Welfare Appendix

Appendix E.1 Alternative Representation of Main Counterfactual Result

Figure E.6 shows the predicted change in sorting patterns in our main counterfactual between 1990 (solid orange) and 2014 (solid blue), compared with the actual change (the corresponding dashed lines) at each household income level between \$25,000 and \$350,000.

Figure E.6: Counterfactual impact of shift in income distribution on the U-shape

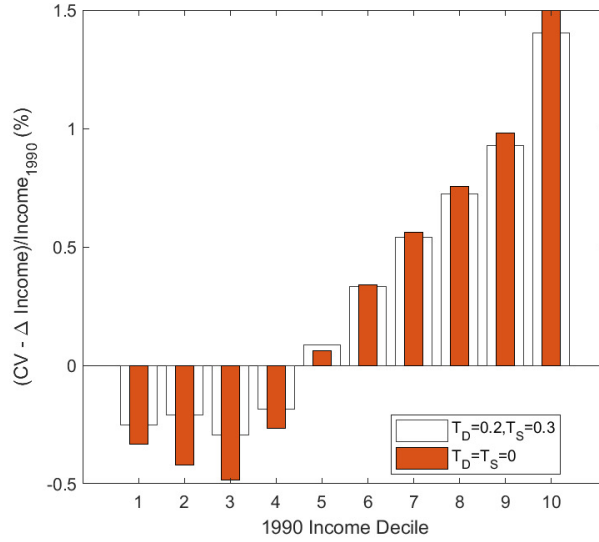


Notes: This figure shows the change in the propensity to live downtown between 1990 (orange) and 2014 (blue) for households in different \$5,000 income brackets between \$25,000 and \$350,000. The solid lines compare the predicted share downtown by income in the model calibrated to the actual data in 1990 to the predicted share downtown that results from the change in the income distribution between 1990 and 2014. The dashed lines compare the share downtown in the data for 1990 and 2014.

Appendix E.2 Importance of Endogenous Public Amenities in Base Specification

As downtown gets richer, taxes collected are higher and public amenities respond for all households downtown. This effect makes both richer and poorer households better off downtown, but housing prices respond to this amenity increase which tends to hurt poorer households. To quantify the net effect, we compute a 1990-2014 counterfactual with no endogenous response in public amenities. Figure E.7 reports the results (red bars), and compares it to the baseline (clear bars). We see that endogenous public amenities tend to mitigate the welfare differential between richer and poorer households somewhat, but are far from strong enough to overturn the general tendency of spatial sorting responses to increase well-being inequality.

Figure E.7: Shutting Down Public Amenities



Appendix E.3 Robustness to Alternate Parameter Values

Which elasticities are important in driving the magnitudes of our distributional welfare results? To explore this question, we examine the sensitivity of our welfare results and changing location choice predictions to alternate parameter values, as summarized in Table E.12. The first three columns report the sensitivity of the absolute change in welfare of the top and bottom decile of the income distribution (columns 1 and 2) and the relative change in welfare between these deciles (column 3) to values of the key parameters, while feeding in the same income shock. The next three columns show the same welfare statistics for renters (i.e., households not receiving any share of the house price appreciation mutual fund). The final columns summarize the model predictions for the urbanization of top income decile households and the suburbanization of bottom income deciles, first in absolute percentage point terms and then as a share of the respective 2.3 percentage point inflow and 4 percentage point outflow observed in the data. Collectively, the results in this table highlight the key mechanisms that are driving our welfare estimates.

Below our baseline results, Table E.12 first shows the sensitivity of these results to ρ , the parameter that governs the strength of non-homotheticity in location choices. We set $\rho = 2$ and $\rho = 4$, which is roughly a two-standard deviation band around our baseline estimates ($\rho = 3$). As individuals get richer, they are more likely to move downtown when ρ is higher. Additionally, the poor are more likely to migrate out in response to the price increase associated with rich moving downtown as ρ is higher. In other words, gentrification forces increase as ρ increases. Therefore, higher values of ρ amplify our welfare results. However, it is interesting to note that, even when $\rho = 2$, accounting for spatial sorting responses increases the inequality between the top and bottom income deciles by 1.45 percentage points (compared to 1.66 percentage points in our baseline specification).

Table E.12: Robustness of Welfare Estimates to Key Parameters

Decile:	$(\Delta CV - \Delta Inc)/Inc_{1990}$						Δ Urban Share			
	All Households			Renters Only			Predicted (p.p.)		Share of Actual	
	Top	Bottom	Diff.	Top	Bottom	Diff.	Top	Bottom	Top	Bottom
Base Specification	1.40	-0.25	1.66	0.77	-0.53	1.30	1.17	-2.32	50%	59%
Elasticity of Substitution between Neighborhood Types (base: $\rho = 3$)										
$\rho = 2$	1.18	-0.27	1.45	0.58	-0.56	1.14	0.87	-2.02	38%	51%
$\rho = 4$	1.64	-0.23	1.87	0.96	-0.49	1.45	1.94	-2.99	84%	76%
Elasticity of Substitution between Same-Type Neighborhoods (base: $\gamma = 6.5$)										
$\gamma = 5$	1.82	-0.14	1.97	1.04	-0.39	1.43	1.87	-3.53	81%	89%
$\gamma = 8$	1.17	-0.30	1.47	0.61	-0.61	1.22	0.95	-1.89	41%	48%
$\gamma = \infty$	0.35	-0.44	0.79	0.03	-0.96	0.99	0.57	-1.03	24%	26%
Elasticity of Substitution between Private Amenities (base: $\sigma = 6.5$)										
$\sigma = 5$	1.55	-0.22	1.77	0.91	-0.50	1.41	1.27	-2.51	55%	63%
$\sigma = 8$	1.32	-0.27	1.59	0.68	-0.55	1.23	1.12	-2.21	48%	56%
$\sigma = \infty$	1.00	-0.35	1.35	0.37	-0.62	0.99	0.97	-1.93	42%	49%
Distance Elasticity of Amenity Consumption (base: $\delta = 0.2$)										
$\delta = 0.1$	1.41	-0.25	1.66	0.77	-0.53	1.30	1.17	-2.31	50%	58%
$\delta = 0.3$	1.40	-0.25	1.65	0.76	-0.53	1.29	1.17	-2.32	51%	59%
Amenity Expenditure Share (base: $\alpha = 0.15$)										
$\alpha = 0.1$	1.39	-0.20	1.58	0.79	-0.41	1.20	1.13	-2.20	49%	56%
$\alpha = 0.3$	1.35	-0.37	1.72	0.64	-0.75	1.39	1.35	-2.72	58%	69%
$\alpha = 0.5$	1.23	-0.47	1.70	0.46	-0.93	1.39	1.69	-3.43	73%	87%
Housing/Land Supply Elasticities (base: $\epsilon_D = 0.6, \epsilon_S = 1.33$)										
$\epsilon_D = 0.1, \epsilon_S = 1.33$	1.40	-0.26	1.66	0.75	-0.55	1.31	1.07	-2.69	46%	68%
$\epsilon_D = \epsilon_S = 1.33$	1.41	-0.23	1.64	0.80	-0.47	1.27	1.30	-1.86	56%	47%
$\epsilon_D = 1.2, \epsilon_S = 2.66$	1.48	-0.08	1.56	0.96	-0.20	1.15	1.27	-2.24	55%	57%
Public Amenity Elasticity (base: $\Omega = 0.05$)										
$\Omega = 0$	1.28	-0.29	1.57	0.64	-0.56	1.21	1.15	-2.26	50%	57%
$\Omega = 0.03$	1.35	-0.27	1.62	0.72	-0.54	1.26	1.16	-2.29	50%	58%
$\Omega = 0.08$	1.48	-0.23	1.71	0.84	-0.51	1.35	1.18	-2.35	51%	59%
Property Tax Rates (base: $T_D = 0.2, T_S = 0.3$)										
$T_D = T_S = 0$	1.50	-0.33	1.84	0.90	-0.67	1.58	1.13	-1.79	49%	45%
$T_D = 0.15, T_S = 0.25$	1.46	-0.25	1.71	0.83	-0.53	1.36	1.18	-2.24	51%	56%
$T_D = 0.25; T_S = 0.25$	1.41	-0.28	1.69	0.79	-0.55	1.34	1.12	-2.25	48%	57%

Next in Table E.12, we show the sensitivity of our results to different values of γ and σ pairs. For lower values of γ or σ , endogenous amplification of amenities downtown is stronger, amplifying the welfare results as is intuitive. As the endogenous amplification of amenities increases, more high income individuals move downtown putting further upward pressure on downtown land prices in both high and low quality neighborhoods. Table E.12 then shows that changing δ has very little effect on our welfare estimates. This is because the share of household spending on non-tradable amenities is relatively small ($\alpha = 0.15$ in our base case). The corresponding channel is therefore quantitatively limited in the model. The higher the value of α , the larger the well-being inequality increase and the higher the endogenous amenity creation, and the more σ and δ matter for our welfare results. In our base calibration, the main love of variety effect at play quantitatively is the on the choice of a neighborhood where to live (governed by γ), rather than on the choice of a neighborhood where to go consume amenities (governed by σ).

Table E.12 then shows that land supply elasticities downtown and in the suburbs are a crucial determinant of the welfare losses to poor renters. This is not surprising. Much of the welfare effect on the poor stems from them paying higher rents downtown as the rich move in. The more inelastic the downtown housing supply (in both absolute terms and relative to the suburbs), the more house prices move, generating modest additional growth in the welfare gap between the poor and the rich. The growth in the welfare gap masks heterogeneity between owners and renters. Additional price growth mitigates welfare losses for poor owners downtown, but exacerbates losses to poor renters. If we simultaneously set $\epsilon_D = \epsilon_S$ to high levels while also setting $\gamma = \sigma = \infty$, there are essentially no welfare changes for any income group stemming from the shifting income distribution over time. As noted above, setting $\gamma = \sigma = \infty$ shuts down the love of variety effects which generates zero welfare gains for high income households while setting the ϵ 's to high values shuts down the housing price effects which leaves welfare unchanged for low income households.

Finally, the response of our welfare estimates to the elasticity of the endogenous component of public amenities confirms that low-income households benefit from the increases in local tax revenues that accompany gentrification. However, as we highlighted in our discussion of Figure E.7 the effects of changing the parameters governing endogenous public amenities on welfare is quantitatively small.

Overall, this variation in our welfare estimates to different parameter values is useful for understanding the forces driving our results. But we note that over reasonable parameter ranges, our welfare results are fairly stable. Our main qualitative results are not reversed by any of these perturbations: poor households (particularly renters) are worse off in both absolute terms and relative to the wealthy from the spatial sorting response to top income growth between 1990 and 2014.

Appendix E.4 Welfare Impact of Alternative Changes to Income and Population

In the analysis above, we have studied the effects of changes in the observed income distribution holding everything else, including population, constant. We complement this analysis by studying

the implication of total population change itself. Further, to tease out what characteristic of the 1990-2014 income shock are important in driving our result, we explore alternative changes in the income distribution.

Table E.13 reports the results. Row 1 re-displays our baseline results. In the second row, we feed in both the actual population change and the change in the income distribution between 1990 and 2014. The third row isolates the effects of population growth separately from income growth, by feeding in only the observed change in population, holding the underlying income distribution constant. Accounting for growth in population results in a larger increase in welfare inequality compared to our baseline. The larger increase stems from two forces. First, population growth amplifies the love of variety effects described above. Second, the increase in population drives up rents everywhere but more so in the downtown areas where land is more constrained. Given our unit housing assumption, this impacts poorer households disproportionately. Changing both population and income increases the well-being gap between high and low income residents by over 5.7 percentage points (on a base of 19 percentage points). Additionally, poorer renters are made worse off in absolute terms by an amount equal to 3.3 percent of their income.

In the fourth row of the table, we return to holding population fixed, and we now assume that all households experience the same income growth equal to the 1990-2014 per capita average. Interestingly, under this alternative income change, the poor are much more worse off in absolute terms relative to our base specification. This happens because a broad based increase in income generates a stronger spatial sorting response, with many middle class individuals in the suburbs moving up their residential Engel curves. This rising demand for downtown living puts more upward pressure on house prices than in our baseline counterfactual, where incomes rise for only a few households at the top of the distribution. As a result, the increase in welfare inequality due to spatial responses is higher with broad based income growth than in our baseline case, at about 2.7 percent (instead of 1.7 percent).

In the final rows (5 through 7) of the table we explore crude predictions about the potential future welfare impact of neighborhood change. Specifically, we hold population growth fixed and ask what happens through the lens of our model when income growth increases by an additional 10, 20, and 30 percent for everyone, starting from the actual 2014 income distribution. These counterfactuals shed some light on the potential effects of future economic growth on the spatial distribution of residents within cities. Holding population fixed, the quantified model suggests that the spatial sorting response from an additional 10 percent income growth for all individuals (which does not impact income inequality) further increases well-being inequality. The mechanisms are the same as what we highlight above. Our model predicts that if income growth in the U.S. continues, even without further increase in income inequality, additional gentrification and within city neighborhood change will be an enduring feature of the urban landscape. This suggests that it is not income inequality per se that drives our results, but instead an increase in the absolute number of high income households regardless of what is happening to the rest of the income distribution.

Before turning to counterfactual policy analysis, we now analyze two counterfactuals that pro-

Table E.13: Welfare Estimates under Different Counterfactual Income Distributions

	$(\Delta CV - \Delta Inc)/Inc_{1990}$						
	Decile:	All Households			Renters Only		
		Top	Bottom	Diff.	Top	Bottom	Diff.
[1] Base Specification (aggregate population fixed)	1.40	-0.25	1.66	0.77	-0.53	1.30	
Alternative Driving Forces (1990-2014)							
[2] Allowing for population growth	4.52	-1.20	5.71	2.49	-3.33	5.82	
[3] Only population growth, no change to income distribution	2.69	-0.96	3.65	1.43	-2.83	4.26	
[4] No population growth, income distribution shifts rightwards	2.08	-0.66	2.74	1.87	-1.41	3.28	
Projected Further Welfare Changes from Further Income Growth from 2014 Onward							
[5] $HHInc_i = HHInc_{i,2014} \times 110\%$	2.98	-1.04	4.02	2.60	-1.98	4.58	
[6] $HHInc_i = HHInc_{i,2014} \times 120\%$	7.80	-2.72	10.52	6.26	-4.82	11.08	
[7] $HHInc_i = HHInc_{i,2014} \times 130\%$	11.39	-4.84	16.22	8.39	-8.93	17.32	

vide additional model validation.

Appendix E.5 Robustness to Alternate Definitions of Neighborhood Quality

Table C.8 shows OLS and IV estimates of ρ for our base specification in column 1 and 2 of Table 1. We show these estimates for different high quality cut-off of our restaurant chain index ranging from 1 to 1.3.⁶¹ We find OLS coefficients ranging from 1.64 to 1.83 that are somewhat smaller than the 2.34 that we obtained for the college share definition. IV estimates are also smaller, ranging from 1.2 to 2.6, but they have weaker first stage and larger standard errors. Table D.10 shows estimates of the amenity demand gravity parameter $\sigma\delta$ using the restaurant quality definition. These estimates are almost identical to those from Table D.9 using the college share quality definition. Finally, Table E.14 replicates the results for our main counterfactual exercise as well as various robustness checks from Table E.12, but using the restaurant quality definition. In all specifications, our welfare results are very similar to those obtained from the college share definition.

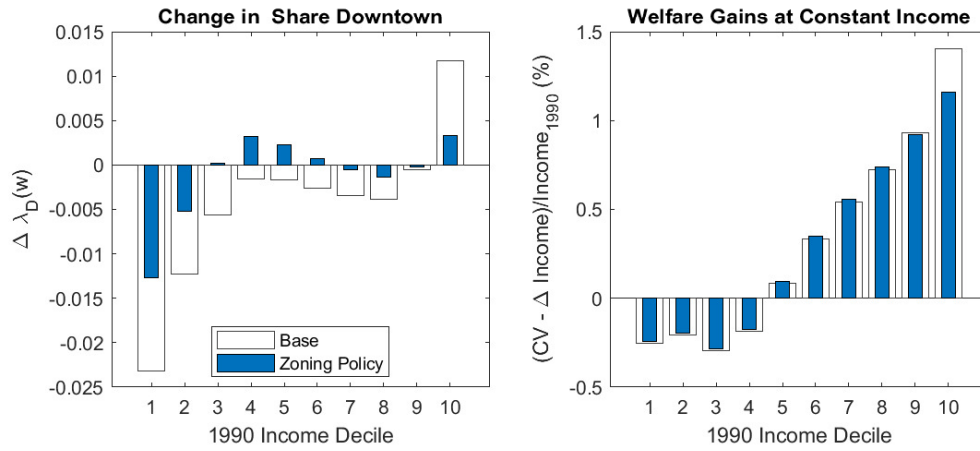
⁶¹Our measure of restaurant quality is not available in 1990, so we impute 2000 tract quality to 1990 tracts.

Table E.14: Robustness of Welfare Estimates to Key Parameters using Restaurant Quality Cutoff

Decile:	$(\Delta CV - \Delta Inc)/Inc_{1990}$						Δ Urban Share			
	All Households			Renters Only			Predicted (p.p.)		Share of Actual	
	Top	Bottom	Diff.	Top	Bottom	Diff.	Top	Bottom	Top	Bottom
Base Specification	1.23	-0.23	1.46	0.66	-0.53	1.18	1.28	-3.00	55%	76%
Elasticity of Substitution between Neighborhood Types (base: $\rho = 3$)										
$\rho = 2$	1.11	-0.25	1.36	0.54	-0.55	1.09	0.90	-2.30	39%	58%
$\rho = 4$	1.41	-0.17	1.57	0.82	-0.48	1.30	2.39	-4.70	103%	119%
Elasticity of Substitution between Same-Type Neighborhoods (base: $\gamma = 6.5$)										
$\gamma = 5$	1.67	-0.03	1.71	1.01	-0.36	1.36	2.53	-6.28	109%	159%
$\gamma = 8$	1.02	-0.28	1.31	0.52	-0.61	1.13	1.00	-2.29	43%	58%
$\gamma = \infty$	0.31	-0.45	0.77	0.01	-0.98	0.99	0.56	-1.10	24%	28%
Elasticity of Substitution between Private Amenities (base: $\sigma = 6.5$)										
$\sigma = 5$	1.38	-0.19	1.57	0.80	-0.50	1.30	1.41	-3.32	61%	84%
$\sigma = 8$	1.14	-0.25	1.39	0.57	-0.54	1.12	1.21	-2.83	52%	72%
$\sigma = \infty$	0.82	-0.34	1.15	0.25	-0.62	0.87	1.01	-2.32	43%	59%
Distance Elasticity of Amenity Consumption (base: $\delta = 0.2$)										
$\delta = 0.1$	1.24	-0.23	1.46	0.66	-0.52	1.19	1.28	-3.00	55%	76%
$\delta = 0.3$	1.22	-0.23	1.45	0.65	-0.53	1.18	1.28	-3.00	55%	76%
Amenity Expenditure Share (base: $\alpha = 0.15$)										
$\alpha = 0.1$	1.21	-0.18	1.39	0.68	-0.40	1.08	1.22	-2.71	53%	68%
$\alpha = 0.3$	1.19	-0.32	1.51	0.55	-0.75	1.29	1.54	-4.09	67%	103%
$\alpha = 0.5$	1.15	-0.34	1.49	0.46	-0.89	1.35	2.17	-6.45	93%	163%
Housing/Land Supply Elasticities (base: $\epsilon_D = 0.6, \epsilon_S = 1.33$)										
$\epsilon_D = 0.1, \epsilon_S = 1.33$	1.23	-0.23	1.46	0.65	-0.54	1.19	1.22	-3.38	53%	85%
$\epsilon_D = \epsilon_S = 1.33$	1.24	-0.21	1.45	0.68	-0.48	1.16	1.36	-2.52	59%	64%
$\epsilon_D = 1.2, \epsilon_S = 2.66$	1.31	-0.05	1.36	0.85	-0.18	1.03	1.35	-2.98	58%	75%
Public Amenity Elasticity (base: $\Omega = 0.05$)										
$\Omega = 0$	1.11	-0.26	1.37	0.54	-0.55	1.09	1.27	-2.98	55%	75%
$\Omega = 0.03$	1.18	-0.24	1.42	0.61	-0.54	1.15	1.28	-2.99	55%	76%
$\Omega = 0.08$	1.30	-0.21	1.51	0.73	-0.51	1.24	1.28	-3.01	55%	76%
Property Tax Rates (base: $T_D = 0.2, T_S = 0.3$)										
$T_D = T_S = 0$	1.24	-0.30	1.54	0.71	-0.65	1.35	1.18	-2.07	51%	52%
$T_D = 0.15, T_S = 0.25$	1.28	-0.22	1.50	0.71	-0.52	1.23	1.27	-2.84	55%	72%
$T_D = 0.25; T_S = 0.25$	1.23	-0.26	1.49	0.68	-0.55	1.23	1.24	-2.99	53%	76%

Appendix E.6 Alternative Policy Counterfactual

Figure E.8: Location Choices and Well-Being under Zoning Policy



Notes: This figure shows the change in the propensity to live downtown (on the left) and change welfare (on the right) that result from the change in the income distribution by income decile. The clear bars show the results from the baseline counterfactual. The blue bars show the results from the alternative counterfactual with zoning that preserves the neighborhood mix (i.e., the share of neighborhoods of each n_j type) at its level from the 1990 equilibrium.